2009

The neurofibromatosis 2 protein, merlin, regulates glial cell growth in an ErbB2- and Src-dependent manner

S. Sean Houshmandi
Washington University School of Medicine
Ryan J. Emnett
Washington University School of Medicine
Marco Giovannini
House Ear Institute, Los Angleles
David H. Gutmann
Washington University School of Medicine

The Neurofibromatosis 2 Protein, Merlin, Regulates Glial Cell Growth in an ErbB2- and Src-Dependent Manner

S. Sean Houshmandi, Ryan J. Emnett, Marco Giovannini and David H. Gutmann

***Mol. Cell. Biol.* 2009, 29(6):1472. DOI: 10.1128/MCB.01392-08.**
Published Ahead of Print 22 December 2008.

MOLECULAR AND CELLULAR BIOLOGY, Mar. 2009, p. 1472–1486 Vol. 29, No. 6
0270-7306/09/$08.00+0 doi:10.1128/MCB.01392-08

The Neurofibromatosis 2 Protein, Merlin, Regulates Glial Cell Growth in an ErbB2- and Src-Dependent Manner[▽]

S. Sean Houshmandi,[1] Ryan J. Emnett,[1] Marco Giovannini,[2] and David H. Gutmann[1]*

Department of Neurology, Washington University School of Medicine, St. Louis, Missouri,[1] and House Ear Institute, Los Angeles, California[2]

Received 4 September 2008/Returned for modification 16 October 2008/Accepted 13 December 2008

Individuals with the inherited cancer predisposition syndrome neurofibromatosis 2 (NF2) develop several central nervous system (CNS) malignancies, including glial cell neoplasms (ependymomas). Recent studies have suggested that the *NF2* protein, merlin (or schwannomin), may regulate receptor tyrosine kinase signaling, intracellular mitogenic growth control pathways, or adherens junction organization in non-nervous-system cell types. For this report, we used glial fibrillary acidic protein conditional knockout mice and derivative glia to determine how merlin regulates CNS glial cell proliferation. We show that the loss of merlin in glial cells results in increased proliferation in vitro and in vivo. Merlin regulation of glial cell growth reflects deregulated Src activity, such that pharmacologic or genetic inhibition of Src activation reduces $Nf2^{-/-}$ glial cell growth to wild-type levels. We further show that Src regulates $Nf2^{-/-}$ glial cell growth by sequentially regulating FAK and paxillin phosphorylation/activity. Next, we demonstrate that Src activation results from merlin regulation of ErbB2 activation and that genetic or pharmacologic ErbB2 inhibition reduces $Nf2^{-/-}$ glial cell Src/Src effector activation and proliferation to wild-type levels. Lastly, we show that merlin competes with Src for direct binding to ErbB2 and present a novel molecular mechanism for merlin regulation of ErbB2-dependent Src signaling and growth control.

Neurofibromatosis type 2 (NF2) is an autosomal dominant inherited cancer syndrome in which affected individuals develop nervous system tumors, including peripheral nerve tumors (schwannomas), leptomeningeal tumors (meningiomas), and glial fibrillary acidic protein (GFAP)-immunoreactive glial cell tumors (spinal ependymomas). NF2 results from a germ line mutation in the *NF2* tumor suppressor gene, located on chromosome 22q (46, 60). Tumors in this disorder arise following somatic inactivation of the one remaining wild-type (WT) *NF2* allele in specific cell types. In this regard, NF2-associated schwannomas, meningiomas, and ependymomas all exhibit biallelic *NF2* gene inactivation (33, 47, 61). In addition, *NF2* gene inactivation is also observed in 50 to 78% of sporadic schwannomas, 32 to 84% of sporadic meningiomas, and 37% of sporadic ependymomas (21, 29), suggesting that this gene is also a key growth regulator in nonhereditary nervous system cancers.

The *NF2* gene was identified in 1993 and found to code for a 595-amino-acid protein, termed merlin or schwannomin (46, 60). Analysis of the predicted protein sequence revealed striking sequence similarity between merlin and a family of protein 4.1 family members that link the actin cytoskeleton to cell surface glycoproteins (55). In particular, merlin most closely resembles the ezrin/radixin/moesin (ERM) subfamily and has been shown to bind actin as well as to associate with several cell surface glycoproteins, including CD44 and β1-integrin (5, 32, 48). However, unlike the ERM proteins, merlin is unique in its capacity to function as a nervous system tumor suppressor gene.

In order to identify the key signaling pathways regulated by the merlin tumor suppressor protein, previous studies have focused on merlin growth regulation in fibroblasts, primary Schwann cell and human schwannoma cell cultures, meningioma and schwannoma tumor cell lines, and other non-central nervous system (non-CNS) cell types. These investigations have resulted in the identification of a large number of non-intersecting growth control pathways regulated by merlin in different cell types. In this regard, merlin has been implicated in epidermal growth factor receptor (EGFR) (9), β1-integrin (15), and CD44 (1, 35, 48) function as well as in Ras (25, 59), Rac1 (34, 52), phosphatidylinositol 3-kinase (44), mitogen-activated protein kinase (MAPK) (7, 30), and STAT (51) intracellular signaling. While each of these pathways is involved in growth control in the brain, it is not known which of these intracellular signaling pathways are deregulated in *NF2*-deficient CNS cell types.

To gain insights into the role of the *NF2* gene in glial cell growth control relevant to the development of targeted therapies for NF2-associated glial cell malignancies, we studied the consequence of merlin loss on the growth of primary brain glial cells (astrocytes) in vitro and in vivo, using *Nf2* conditional knockout genetically engineered mice (GEM). We demonstrate for the first time that merlin regulates brain glial cell growth by controlling the phosphorylation/activity of Src and its downstream effectors, FAK and paxillin. Furthermore, we show that merlin regulation of Src phosphorylation/activation is modulated by ErbB2 phosphorylation/activation and ErbB2-Src binding. Finally, we show that merlin competitively inhibits Src binding to ErbB2 and, in this manner, prevents ErbB2-mediated Src phosphorylation and downstream mitogenic signaling. Based on these findings, we propose a novel mechanism for merlin growth regulation in CNS glia.

* Corresponding author. Mailing address: Department of Neurology, Washington University School of Medicine, Box 8111, 660 South Euclid Avenue, St. Louis, MO 63110. Phone: (314) 362-7379. Fax: (314) 362-2388. E-mail: gutmannd@neuro.wustl.edu.

▽ Published ahead of print on 22 December 2008.

MATERIALS AND METHODS

Cell culture. Forebrain glial cell cultures from postnatal day 3 *Nf2*$^{flox/flox}$ mice (18) were generated as previously described (24, 49). Briefly, forebrains were isolated and enzymatically digested with 0.25% trypsin for 10 min at 37°C. Cells were then placed in modified Eagle's medium with 10% fetal bovine serum and grown for 2 weeks to generate cultures composed of >97% GFAP-immunoreactive cells (glia). Adenovirus type 5 (Ad5) viruses, namely, Ad5-LacZ and Ad5-Cre (University of Iowa Gene Transfer Core, Iowa City, IA), were used to produce control (WT) and *Nf2*-deficient (*Nf2*$^{-/-}$) glia, respectively, according to protocols described previously in our laboratory (10, 49). Merlin loss was confirmed by immunoblot analysis using a rabbit polyclonal *NF2* antibody (NF2 C-18; Santa Cruz Biotechnology, Santa Cruz, CA) (1:1,000 dilution) or the laboratory-generated WA30 antibody (50) (1:2,000 dilution).

Pharmacological inhibitors. Glial cell cultures were treated with the following experimentally determined concentrations of inhibitors for 24 h prior to all analyses: Src inhibitor PP2, 0.5 nM (Calbiochem, San Diego, CA); ErbB2 inhibitor AG825, 4.0 μg/ml (Calbiochem); FAK/paxillin inhibitor echistatin, 2.0 μg/ml (Sigma, St. Louis, MO).

shRNA constructs and lentiviral delivery. Mouse gene-specific lentiviral plasmids for *Src* (GenBank accession no. NM_009271; TRCN0000023595 and TRCN0000023598), *Fak* (NM_007982), *paxillin* (NM_133915), and *ErbB2* (NM_109715) small hairpin RNAs (shRNAs) were commercially purchased (Sigma). Corresponding lentiviruses were produced as previously described (54), and the most effective silencing construct was selected for further study. Briefly, 293T cells were transfected with Src.shRNA, FAK.shRNA, Pxn.shRNA, and ErbB2.shRNA lentiviral plasmids or a control vector (pLKO1-GFP plasmid; courtesy of Sheila Stewart, Washington University), using Fugene HD (Roche, Mannheim, Germany). Lentiviruses were harvested at 48 and 72 h posttransfection. WT and *Nf2*$^{-/-}$ glia were infected for a total of 48 h. WT and *Nf2*$^{-/-}$ glia were serum starved for 24 h prior to each experiment.

Thymidine incorporation assay. Glial cells were seeded at 5×10^4 cells per well for 24 h of serum starvation. [^{3}H]thymidine (1 μCi per well) was added in serum-free medium, and the number of counts per minute was determined after 24 h.

Cell attachment, apoptosis, and cell adhesion. Cell attachment was measured by seeding 5×10^4 *Nf2*$^{flox/flox}$ glial cells treated with Ad5-LacZ (WT) and Ad5-Cre (*Nf2*$^{-/-}$) into 96-well plates precoated with 10 μg/ml fibronectin (Gibco) following 24 h in serum-free medium. After 4 hours, the wells were washed with 1× phosphate-buffered saline (PBS) and incubated in 0.5% crystal violet for 30 min. The number of attached cells was determined by extraction in 1% sodium dodecyl sulfate (SDS) overnight and spectrophotometric analysis at 540 nm.

Apoptosis was measured by seeding WT and *Nf2*$^{-/-}$ glial cells into 24-well plates, followed by preincubation in serum-free medium in the presence and absence of 5 nM staurosporine (Sigma) for 24 h. Cells were then immunostained with cleaved caspase-3 antibody (1:500 dilution; Cell Signaling Technology) and 1% bis-benzimide–PBS solution. The number of apoptotic cells was determined by the fraction of caspase-3-positive cells relative to the total number of DAPI (4′,6-diamidino-2-phenylindole)-positive cells. Terminal deoxynucleotidyltransferase-mediated dUTP-biotin nick end labeling (TUNEL) was also used to detect apoptosis levels in vivo. TUNEL labeling of *Nf2*^{GFAP}CKO and *Nf2*$^{flox/flox}$ mouse brain sections was performed using a commercially available fluorescein-based in situ cell death detection kit (Roche) according to the manufacturer's instructions. The number of TUNEL-positive cells in the hippocampus was determined by direct cell counting.

The formation of adherens junctions was assessed by β-catenin immunostaining as previously described (28). WT and *Nf2*$^{-/-}$ glial cells were grown to confluence and serum starved for 24 h. The cells were then permeabilized and fixed by incubation in 3% paraformaldehyde–0.1% Triton X-100 in PBS for 10 min. Cells were blocked in PBS plus 10% goat serum and incubated with anti-β-catenin antibodies (1:200 dilution; Chemicon) and then with secondary antibody (1:200 dilution; Alexa). A 1.0% bis-benzimide solution was used to counterstain nuclei. Images were acquired on an inverted fluorescence microscope (Eclipse TE300 inverted microscope; Nikon, Japan) equipped with a digital camera (Optronics, Goleta, CA).

Merlin reexpression. To reintroduce merlin into WT and *Nf2*-deficient glia, murine stem cell virus (MSCV) retroviral transduction was used to express either WT merlin or an inactive mutant merlin protein containing a nonfunctional patient missense mutation (L64P), as previously described (49, 62). MSCV-merlin and MSCV-merlin-L64P viral constructs were generated by cloning the human *NF2* cDNA into the MSCV-green fluorescent protein (MSCV-GFP) vector. MSCV-merlin, MSCV-merlin-L64P, and the control (empty MSCV-GFP vector) retrovirus were generated in 293T cells. Transduced glia were evaluated by fluorescence microscopy using a microscope equipped with a digital camera. More than 90% of glial cells displayed GFP expression, indicative of effective transduction. Merlin expression was confirmed by immunoblotting with a commercially available merlin antibody (NF2 C-18; 1:1,000 dilution).

Immunoblotting. Untreated or reagent-treated primary glia and brains were lysed in NP-40 lysis buffer (50 mM Tris [pH 7.0], 150 mM NaCl, 0.5% NP-40, 1 mM dithiothreitol [DTT]) with protease inhibitors (leupeptin, benzamidine, aprotinin, and phenylmethylsulfonyl fluoride). Proteins were separated by SDS-polyacrylamide gel electrophoresis (SDS-PAGE) and transferred to polyvinylidene difluoride membranes (Millipore, Billerica, MA) prior to detection with antibodies against phosphorylated Src-Y416, FAK-Y576/577 (Cell Signaling Technology, Beverly, MA) (1:1,000 dilution), ErbB2-Y877 (Abcam, Cambridge, MA) (1:1,000 dilution), and paxillin-Y118 (Cell Signaling Technology, Beverly, MA) (1:1,000 dilution). Antibodies against total Src, FAK, ErbB2, and paxillin (from the same manufacturers and at the same dilutions as the phospho-specific antibodies), as well as α-tubulin (Sigma) (1:5,000 dilution), were used as controls for equal protein loading and quantitation. Antibodies against phosphorylated MAPK p44/p42, AKT-T308, and EGFR-Y845 as well as total MAPK p44/p42, AKT, and EGFR were purchased from Cell Signaling Technology and used at a 1:1,000 dilution. Densitometric analysis was performed using Gel-Pro Analyzer 4.0 software (MediaCybernetics, Silver Spring, MD) with anti-tubulin or non-phospho-Src, -paxillin, -FAK, and -ErbB2 antibodies as internal loading controls.

Immunoprecipitation. Primary glia were lysed by sonication in precipitation lysis buffer (20 mM Tris [pH 7.5], 150 mM NaCl, 1 mM EDTA, 1 mM EGTA, 1% Triton X-100, 2.5 mM sodium pyrophosphate, 1 mM beta-glycerophosphate, 1 mM Na_3VO_4, 1 mg/ml leupeptin, 1 mM phenylmethylsulfonyl fluoride). Antibodies against Src (U.S. Biological) (1:100 dilution) or ErbB2 (Upstate, Temecula, CA) (1:100 dilution) were added to the lysates and incubated with gentle rocking overnight at 4°C. Protein A-agarose beads (Calbiochem) were then added to the mixture and rotated for 4 hours. Beads were washed with precipitation lysis buffer and resuspended in 2× Laemmli buffer. Each sample was then boiled and resolved by SDS-PAGE, followed by immunoblot analysis as described above.

Tyrosine phosphorylation was detected following incubation of cell lysates with agarose-conjugated monoclonal anti-phosphotyrosine (PY20) antibody (Sigma) according to the manufacturer's protocols. Following washes, proteins were eluted by boiling in gel loading buffer and detected by immunoblotting using antibodies against Ack1 (Cell Signaling Technology) (1:1,000 dilution), p130CAS (Sigma) (1:1,000 dilution), CASPR (Santa Cruz Biotechnology) (1:500 dilution), ErbB3 (Cell Signaling Technology) (1:1,000 dilution), and ErbB4 (Cell Signaling Technology) (1:1,000 dilution).

Src and ErbB2 kinase activity assays. Primary glial cells were lysed by sonication in precipitation lysis buffer. Antibodies against Src (Cell Signaling) (1:50 dilution) or ErbB2 (Cell Signaling) (1:50 dilution) were added to the lysates and incubated with gentle rocking overnight at 4°C. Protein G agarose beads (Calbiochem) were then added to the mixture and rotated overnight. Beads were washed and resuspended in 50 μl of 1× kinase buffer containing signal transduction protein Tyr160-biotinylated peptide substrate (1.5 μM; Cell Signaling), 20 μM ATP, and 1.25 μM DTT for Src or FLT3 Tyr589-biotinylated peptide (1.5 μM; Cell Signaling), 20 μM ATP, and 1.25 μM DTT for ErbB2. After 30 min, each reaction was stopped by the addition of EDTA. Twenty-five microliters of each reaction mix was added to a 96-well streptavidin-coated plate containing 75 μl distilled H_2O/well and incubated at room temperature for 60 min. After the plates were washed with PBS-Tween 20 (PBS-T), 100 μl of diluted detection antibody (phosphotyrosine monoclonal antibody [MAb] P-Tyr-100 [1:500 dilution] in PBS-T with 1% bovine serum albumin) was added to each well for 2 h at 37°C. Next, 100 μl of horseradish peroxidase-labeled mouse secondary antibody (1:500 in PBS-T with 1% bovine serum albumin; Cell Signaling) was added, and the plates were incubated at room temperature for 30 min, washed with PBS-T, and developed in 100 μl TMB solution (Cell Signaling) for 10 min at 37°C. Following the addition of stop solution (Cell Signaling), the absorbance was read at 450 nm.

Rac1 activation assay. Rac activation in WT and *Nf2*$^{-/-}$ glial cell lysates was determined using a Rac1 activation assay kit (Upstate Biotechnologies, Temecula, CA) according to the manufacturer's instructions, as previously described (17).

In vitro binding assays. A commercially available TnT quick coupled transcription/translation system (Promega, Madison, WI) was used as previously described (20) to transcribe and translate WT merlin (NF2.WT), mutant merlin (NF2.L64P), a C-terminal merlin fragment containing residues 300 to 595 (NF2.C-term), an N-terminal merlin fragment containing residues 1 to 300 (NF2.N-term), a merlin fragment containing residues 300 to 557 (NF2.300-557), and WT Src (Src) in the

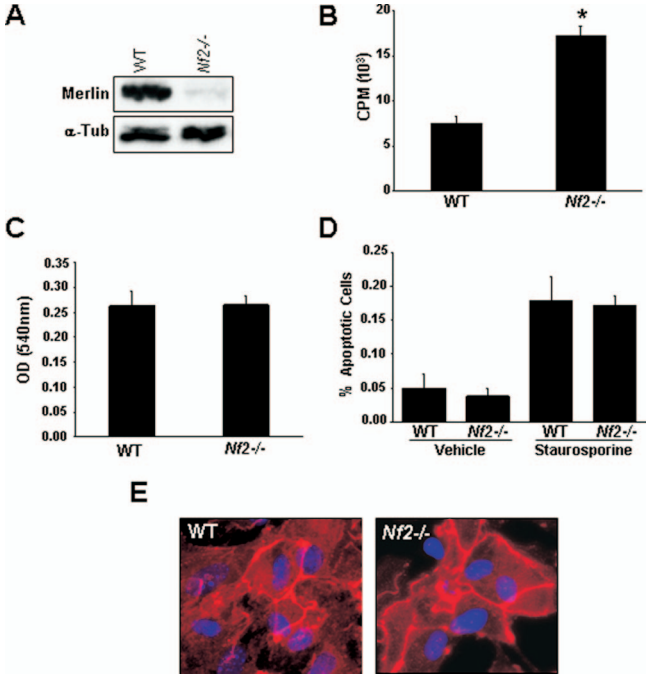

FIG. 1. Merlin regulates glial cell growth in vitro. (A) Immunoblot analysis of merlin expression in primary glial cell lysates demonstrates a >95% reduction in merlin expression in $Nf2^{-/-}$ glia (Ad5-Cre treatment) relative to that in WT glia (Ad-LacZ treatment), as assessed by scanning densitometry. α-Tub, α-tubulin. (B) $Nf2^{-/-}$ glia exhibited a 2.3-fold increase in proliferation relative to WT glia, as determined by [^{3}H]thymidine incorporation. *, $P < 0.001$ (unpaired t test). (C) WT and $Nf2^{-/-}$ glial cells were seeded in fibronectin-coated plates, and the number of adherent cells was determined using a spectrophotometric assay. No differences in cell attachment were observed between WT and $Nf2^{-/-}$ glial cells. OD, optical density. (D) WT and $Nf2^{-/-}$ glial cells were immunostained with cleaved caspase-3 antibody in the presence and absence of staurosporine (5 nM). No differences in apoptosis were observed between WT and *Nf2*-deficient glial cells in either the presence or absence of staurosporine. (E) β-Catenin staining along cell contact junctions in WT and $NF2^{-/-}$ glial cells revealed similar patterns by immunofluorescence microscopy.

presence of 2 μCi [^{35}S]methionine (1,000 Ci/mmol at 10 mCi/ml; Perkin-Elmer, Waltham, MA). The first set of experiments were direct binding experiments in which 75% of each TnT preparation containing radiolabeled merlin or Src was incubated with 1.0 μg recombinant His-tagged ErbB2 or Src protein (Invitrogen, Carlsbad, CA) overnight at 4°C. ErbB2.His/merlin, ErbB2.His/Src, and Src.His/merlin reaction mixtures were then incubated with His-Select nickel affinity gel (Sigma) for 4 h at 4°C. The nickel affinity gel was washed and eluted with 2× Laemmli buffer. Bound proteins along with the remaining original 25% of each TnT reaction mixture were then separated by SDS-PAGE and analyzed by autoradiography. Densitometric analysis was performed using Gel-Pro Analyzer 4.0 software (MediaCybernetics), with 25% of each TnT preparation serving as the input control for normalization. The second set of experiments were competition binding assays in which 1.0 μg of recombinant His-tagged ErbB2 protein was incubated with radiolabeled Src in the presence of increasing amounts of nonradiolabeled in vitro TnT-generated merlin or merlin fragments (none or a 1×, 5×, or 10× excess of merlin or merlin fragments relative to Src). Complementary experiments using increasing amounts of nonradiolabeled Src (none or a 1×, 5×, or 10× excess of Src relative to merlin) were also performed. As described above, each reaction mix was incubated with His-Select nickel affinity gel, followed by SDS-PAGE, autoradiography, and densitometric analyses.

In vivo Src inhibition. $Nf2^{GFAP}$CKO mice were generated by successive intercrossing of $Nf2^{flox/flox}$ and $Nf2^{flox/wt}$; *GFAP-Cre* mice, and merlin expression in the brain was detected by Western blotting using merlin antibodies (NF2 C-18; 1:1,000 dilution). Ten-day-old $Nf2^{flox/flox}$ (WT) and $Nf2^{GFAP}$CKO ($Nf2^{-/-}$) mice ($n = 4$ per experimental group) received 2 mg/kg of body weight of PP2 (Cal-

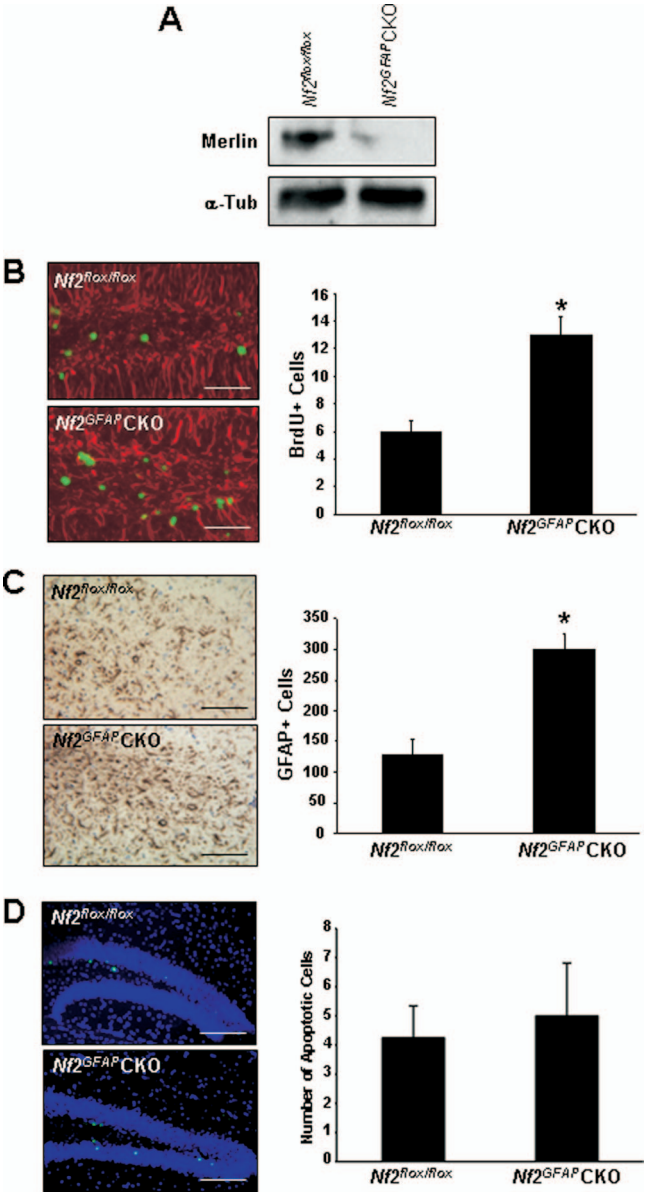

FIG. 2. Merlin regulates glial cell growth in vivo. (A) Immunoblot analysis of merlin expression in $Nf2^{flox/flox}$ and $Nf2^{GFAP}$CKO mouse brain lysates also demonstrates a >90% reduction in merlin expression in $Nf2^{GFAP}$CKO mice, as assessed by scanning densitometry. α-Tub, α-tubulin. (B) Representative immunofluorescence photomicrographs of hippocampi from BrdU-injected $Nf2^{flox/flox}$ and $Nf2^{GFAP}$CKO mice labeled with both BrdU (green) and GFAP (red) antibodies. $Nf2^{GFAP}$CKO mouse brains had 2.2-fold more BrdU-positive cells than $Nf2^{flox/flox}$ mouse brains. *, $P < 0.001$ (unpaired t test). (C) Representative photomicrographs of hippocampi from $Nf2^{flox/flox}$ and $Nf2^{GFAP}$CKO mice labeled with GFAP antibodies. $Nf2^{GFAP}$CKO mouse brains had a 2.4-fold increase in the number of GFAP-expressing cells compared to $Nf2^{flox/flox}$ mouse brains. *, $P = 0.001$ (unpaired t test). (D) Representative photomicrographs of in vivo TUNEL staining of hippocampi from $Nf2^{flox/flox}$ and $Nf2^{GFAP}$CKO mouse brains, revealing no significant differences in the number of apoptotic cells between $Nf2^{GFAP}$CKO and $Nf2^{flox/flox}$ mice.

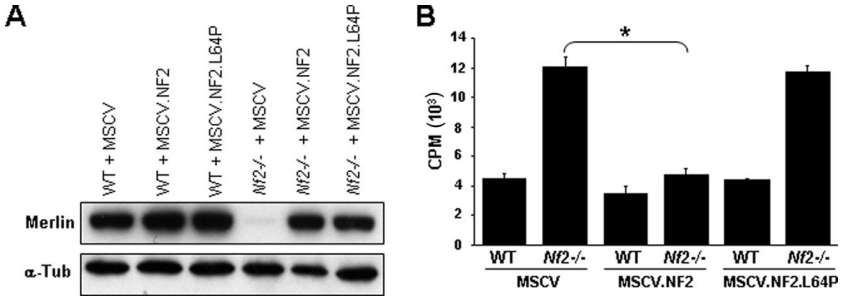

FIG. 3. Expression of WT but not mutant merlin reduces $Nf2^{-/-}$ glial cell proliferation in vitro. (A) Immunoblot analysis of merlin expression in WT and $Nf2^{-/-}$ glia infected with empty MSCV, MSCV containing WT merlin (MSCV.NF2), or MSCV containing mutant merlin (MSCV.NF2.L64P). α-Tubulin (α-Tub) protein expression was used as an internal control for equal protein loading in all Western blot analyses. (B) Merlin reintroduction reduces the increased proliferation observed in $Nf2^{-/-}$ glia to WT levels, whereas the reintroduction of mutant (L64P) merlin has no effect. *, $P < 0.003$ (unpaired t test).

biochem) in dimethyl sulfoxide or the same volume of dimethyl sulfoxide alone by intraperitoneal injection three times a week for 2 weeks, as previously described (15).

Immunohistochemistry. To analyze proliferation in vivo, 7- to 10-day-old $Nf2^{flox/flox}$ and $Nf2^{GFAP}$CKO mice ($n = 3$) were injected with 5-bromo-2-deoxyuridine (BrdU; Sigma) (50 μg/g of body weight) as previously described (24). After 2 hours, mice were euthanized and their brains were removed. A quarter of each brain was separated for immunoblot analyses, and the remainder of each brain was fixed in 4% paraformaldehyde and paraffin sections prepared. Brain sections were immunolabeled with BrdU (Abcam, Cambridge, MA) (1:100 dilution) and GFAP (Sigma) (1:200 dilution) antibodies followed by Alexa 488 (BrdU; Abcam) (1:200 dilution)- and Cy3 (GFAP; Sigma) (1:500 dilution)-conjugated secondary antibodies. All sections were photographed with a digital camera (Optronics) attached to an inverted microscope (Nikon). The number of BrdU-positive cells in the hippocampus for each set of three littermates was determined by direct cell counting.

To quantitate glial cell numbers in vivo, GFAP immunohistochemistry (Sigma) (1:200 dilution) with Vectastain ABC development (Vector Laboratories, Burlingame, CA) was performed as previously reported (2). The number of GFAP-positive cells in the hippocampus for each set of three littermates was determined by direct cell counting.

RESULTS

Merlin regulates glial cell growth in vitro and in vivo. To study merlin growth regulation in CNS glia, we employed primary neonatal forebrain glial cultures from *Nf2* conditional knockout ($Nf2^{flox/flox}$) mice, in which the expression of merlin is eliminated by adenoviral delivery of Cre recombinase (Ad-Cre). Following Cre recombinase transduction, $Nf2^{-/-}$ ($Nf2^{flox/flox}$ + Ad-Cre) glia consistently demonstrated a >95% decrease in merlin expression compared to $Nf2^{flox/flox}$ glia transduced with Ad-LacZ virus (WT) (Fig. 1A). As previously reported for other cell types, $Nf2^{-/-}$ glia exhibited a 2-fold increase in proliferation compared to WT glia by thymidine incorporation assay (mean = 2.3-fold increase) (Fig. 1B). Identical results were obtained using BrdU incorporation in vitro (data not shown). In contrast, $Nf2^{-/-}$ glia were indistinguishable from WT glia with respect to cell attachment (Fig. 1C), apoptosis (Fig. 1D), and adherens junctions (Fig. 1E).

To determine whether our findings using *Nf2*-deficient glia in vitro were also observed in the intact brain in vivo, we analyzed glial cell proliferation in $Nf2^{GFAP}$CKO mice. $Nf2^{GFAP}$CKO mice were generated by the successive intercrossing of $Nf2^{flox/flox}$ mice with $Nf2^{flox/wt}$; *GFAP-Cre* mice to yield mice with *Nf2* loss in GFAP-expressing cells (glia). $Nf2^{GFAP}$CKO mice were born at the expected Mendelian frequencies, were phenotypically normal, and demonstrated a

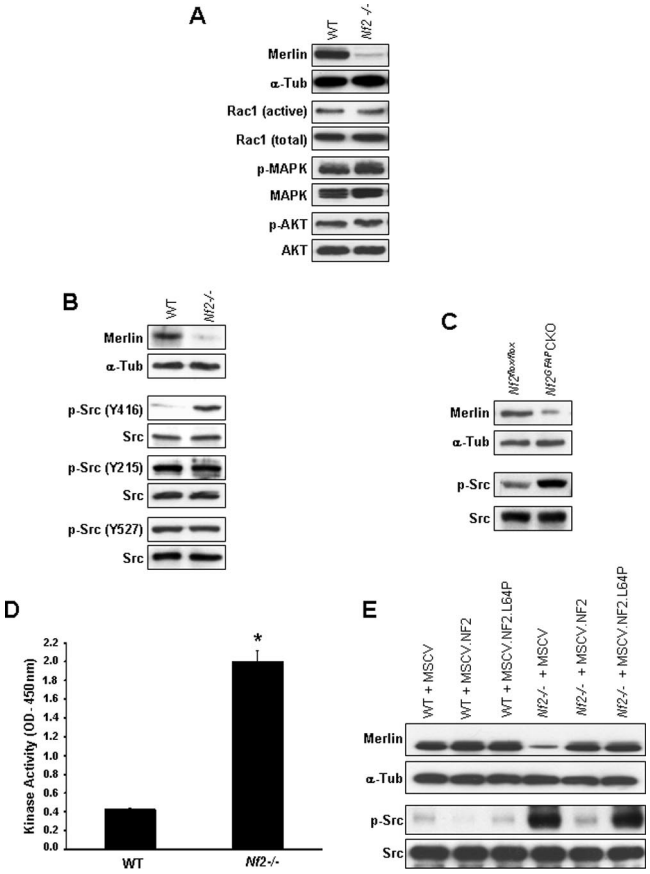

FIG. 4. Merlin regulates Src activation in $Nf2^{-/-}$ glial cells. (A) Rac1 activation assay shows similar Rac1 activities in WT and $Nf2^{-/-}$ glial cell lysates. Immunoblot analyses using phospho-specific MAPK and AKT antibodies demonstrated no change in MAPK or AKT activation in $Nf2^{-/-}$ glia compared to WT glia in vitro. Total Rac1, MAPK, and AKT expression levels were used as internal controls for equal protein loading. α-Tub, α-tubulin. (B) Immunoblot analysis of Src activation in WT and *Nf2*-deficient ($Nf2^{-/-}$) glia, using phospho-specific Src antibodies (specific for phosphorylation at Y416, Y215, and Y527). $Nf2^{-/-}$ glia exhibited a 6.7-fold increase in Src activation at tyrosine 416 compared to WT glia, with no change in Src phosphorylation at tyrosine 215 or tyrosine 527. (C) $Nf2^{GFAP}$CKO mouse brains also show increased activation of Src (2.9-fold) compared to $Nf2^{flox/flox}$ mouse brains, as assessed by immunoblot analyses and scanning densitometry. (D) In a Src kinase activity assay, $Nf2^{-/-}$ glia exhibited a 4.7-fold increase in Src activity relative to WT glia. *, $P < 0.001$ (unpaired t test). OD, optical density. (E) WT but not mutant merlin reduces Src activation in $Nf2^{-/-}$ glia.

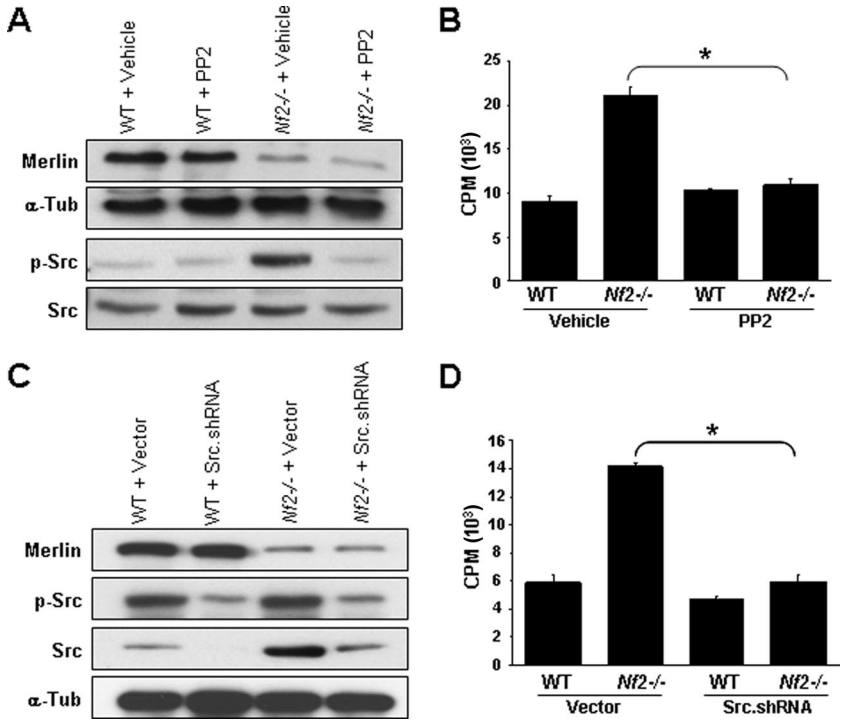

FIG. 5. Src inhibition restores $Nf2^{-/-}$ glial cell proliferation to WT levels in vitro. (A) The PP2 Src inhibitor blocks Src activation in $Nf2^{-/-}$ glia. (B) PP2 treatment eliminates the growth advantage observed in $Nf2^{-/-}$ glia, as measured by [^{3}H]thymidine incorporation. *, $P < 0.001$ (unpaired t test). (C) Immunoblot analysis of Src expression and activation in WT and $Nf2^{-/-}$ glia following infection with Src.shRNA or vector (pLK01-GFP) demonstrates >90% inhibition of Src expression and activation after Src.shRNA treatment, as assessed by scanning densitometry. Total Src or tubulin (α-Tub) protein expression was used as an internal control for equal protein loading. (D) Src.shRNA treatment eliminates the growth advantage observed in $Nf2^{-/-}$ glia, as measured by [^{3}H]thymidine incorporation *, $P < 0.001$ (unpaired t test).

>90% decrease in merlin expression in the brain compared to $Nf2^{flox/flox}$ mice (Fig. 2A). Despite efficient *Nf2* inactivation in glia throughout the neuroaxis, these mice did not develop nervous system tumors, even after 15 months of age ($n = 15$ mice to date).

To measure glial cell proliferation in vivo, postnatal day 10 $Nf2^{GFAP}$CKO pups were injected with BrdU, and the numbers of BrdU- and GFAP-positive glia were quantitated. Consistent with our findings in vitro, we observed a 2-fold increase in the numbers of BrdU-positive cells and GFAP-expressing cells in $Nf2^{GFAP}$CKO mice compared to those in $Nf2^{flox/flox}$ controls (mean = 2.2- and 2.4-fold increases, respectively) (Fig. 2B and C). No in vivo changes in apoptosis were observed in the hippocampus for $Nf2^{GFAP}$CKO mice compared to $Nf2^{flox/flox}$ controls (Fig. 2D).

To demonstrate that the observed increase in cell proliferation was directly related to merlin expression, we restored merlin expression in *Nf2*-deficient glia by MSCV retroviral transduction. For these experiments, we reintroduced either WT merlin (NF2) or an inactive merlin protein containing a nonfunctional patient missense mutation (NF2.L64P) (4) into WT and $Nf2^{-/-}$ glia. Following transduction, the levels of merlin expression in $Nf2^{-/-}$ glia were similar to those observed in WT glia (Fig. 3A). Consistent with the notion that merlin directly regulates cell growth in glia, the reintroduction of WT but not mutant merlin reduced the proliferation of $Nf2^{-/-}$ glia to the levels observed in WT glia (Fig. 3B). No effect of merlin expression was observed on WT glial cell proliferation. Collectively, these results demonstrate that merlin is a direct regulator of glial cell growth in vitro and in vivo.

Merlin regulates glial cell growth in a Src-dependent fashion. Previous studies using different primary cell types and established cell lines have shown that merlin regulates several distinct signaling pathways. To identify the signaling pathway responsible for merlin growth regulation in glia, we employed activity assays and activation (phospho-)specific antibodies to determine which of these previously implicated NF2-associated signaling pathways were deregulated in $Nf2^{-/-}$ glia. In contrast to previous reports using non-CNS cell types, no changes in Rac1, MAPK, and AKT activation were observed in $Nf2^{-/-}$ compared to WT glia (Fig. 4A). However, we found that $Nf2^{-/-}$ glia exhibited hyperphosphorylation of the Src nonreceptor tyrosine kinase oncoprotein on tyrosine 416, a residue located within the Src kinase domain activation loop (45) (Fig. 4B). No changes in Src phosphorylation were seen on another common activation site (tyrosine 215) or on the deactivation site (tyrosine 527). We also examined Src phosphorylation in lysates from $Nf2^{GFAP}$CKO mice and found that Src tyrosine 416 phosphorylation was likewise increased in $Nf2^{GFAP}$CKO mice relative to that in control mice in vivo (Fig. 4C). To directly demonstrate that Src activity was increased in $Nf2^{-/-}$ glia, we assayed Src activity following Src immunoprecipitation. Similar to the results obtained with the Src Y416 phospho-antibody, we observed a 4.7-fold increase in Src activity in $Nf2^{-/-}$ glia relative to that in their WT counterparts (Fig. 4D). Finally, to demonstrate that merlin directly regulates

Src activity, we assessed Src Y416 phosphorylation following the reexpression of merlin. In these experiments, WT but not mutant (NF2.L64P) merlin reexpression in *Nf2*$^{-/-}$ glia resulted in a reduction of Src Y416 phosphorylation to the levels observed in WT glia (Fig. 4E).

To determine whether Src hyperactivation resulting from merlin loss was responsible for the increased proliferation seen in *Nf2*-deficient glia, we treated WT and *Nf2*$^{-/-}$ cells with PP2, a potent inhibitor of the Src family of kinases (23). PP2 treatment resulted in a >90% reduction in Src activity, as assessed using Src phospho-specific antibodies (Fig. 5A), and was sufficient to reduce the proliferation of *Nf2*$^{-/-}$ glia to WT levels (Fig. 5B). No effect of PP2 treatment on WT glial cell proliferation was observed. To complement these findings, we utilized shRNA interference to silence Src expression. *Nf2*$^{-/-}$ glia infected with Src.shRNA lentivirus exhibited a >90% reduction in Src expression, as assessed using total and Src activation-specific antibodies (Fig. 5C), and similar to the case for PP2 treatment, the shRNA decreased *Nf2*$^{-/-}$ glial cell proliferation to WT levels (Fig. 5D). Similar results were obtained using a second, independent Src.shRNA lentivirus (data not shown). In all cases, no effect of Src.shRNA on WT glial cell proliferation was observed. Together, these results demonstrate that merlin regulation of glial cell growth requires Src Y416 phosphorylation and activation.

Src-mediated merlin regulation of glial cell growth requires FAK and paxillin. To determine how Src regulates glial cell growth, we next examined the activation of known Src downstream effector molecules, including FAK, paxillin, p130CAS, Ack1, and CASPR. While we found no change in the phosphorylation status of p130CAS, Ack1, and CASPR in *Nf2*$^{-/-}$ versus WT glia (Fig. 6A), we found increased FAK tyrosine 576/577 and paxillin tyrosine 118 phosphorylation in *Nf2*$^{-/-}$ glia relative to their WT counterparts (Fig. 6B, left panels). Similarly, immunoblot analysis of *Nf2*^{GFAP}CKO mouse brain lysates demonstrated increased FAK and paxillin phosphorylation relative to that in control littermates (Fig. 6B, right panels).

To demonstrate that merlin loss and Src activation were directly responsible for the increases in FAK and paxillin phosphorylation, we transduced WT and *Nf2*$^{-/-}$ glia with WT or mutant (L64P) merlin, using MSCV retroviral delivery. In these experiments, reexpression of WT but not mutant merlin in *Nf2*$^{-/-}$ glia reduced FAK and paxillin phosphorylation to WT levels (Fig. 6C). To demonstrate that Src activation was responsible for FAK and paxillin activation in *Nf2*$^{-/-}$ glial cells, we employed PP2 pharmacologic Src inhibition and shRNA Src silencing (Src.shRNA). Both PP2 (left panels) and Src.shRNA (right panels) inhibition reduced FAK and paxillin phosphorylation in *Nf2*$^{-/-}$ glial cells to WT levels (Fig. 6D). No effect of merlin expression, PP2 treatment, or Src.shRNA lentiviral infection was observed on FAK and paxillin phosphorylation in WT glia.

To determine whether FAK and paxillin were responsible for the increased proliferation observed in *Nf2*-deficient glia, we initially used a known FAK/paxillin pharmacological inhibitor, echistatin (11). Treatment of *Nf2*$^{-/-}$ glia with echistatin resulted in inhibition of FAK and paxillin phosphorylation but had no effect on Src phosphorylation (Fig. 7A, upper panel). Furthermore, echistatin treatment reduced the proliferation of

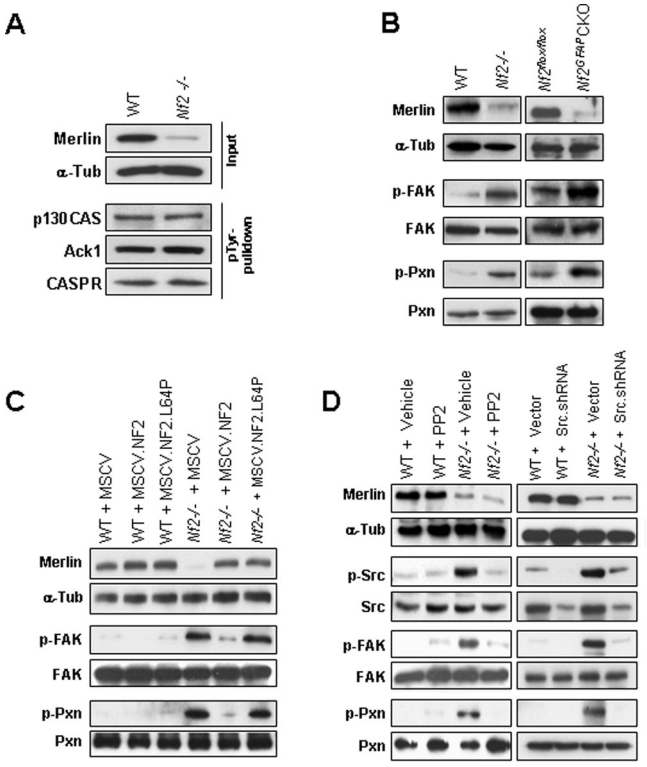

FIG. 6. Merlin regulates phosphorylation of the Src effectors FAK and paxillin. (A) Immunoblot analyses of WT and *Nf2*$^{-/-}$ glial lysates following phosphotyrosine (pTyr) affinity binding with antibodies against p130CAS, Ack1, and CASPR show no change in the phosphorylation state of these Src effectors. Merlin and α-tubulin (α-Tub) expression levels are included as internal controls. (B) *Nf2*-deficient (*Nf2*$^{-/-}$) glia demonstrated a 4.9-fold increase in FAK (Y576/577) phosphorylation and a 5.5-fold increase in paxillin (Pxn) phosphorylation (Y118) (left). *Nf2*^{GFAP}CKO mouse brains also showed increased activation of FAK (2.2-fold) and paxillin (2.5-fold) compared to *Nf2*$^{flox/flox}$ mouse brains, as assessed by immunoblot analyses and scanning densitometry (right). (C) WT but not mutant merlin inhibits both FAK and paxillin phosphorylation in *Nf2*$^{-/-}$ glia. (D) The Src inhibitor PP2 (left) as well as Src.shRNA silencing (right) reverses the hyperphosphorylation of both FAK and paxillin in *Nf2*$^{-/-}$ glia.

Nf2$^{-/-}$ glia to WT levels (Fig. 7A, lower panel). No effect of echistatin treatment on WT glial cell proliferation was observed. We next performed complementary experiments using specific FAK (FAK.shRNA) and paxillin (Pxn.shRNA) shRNA reagents to circumvent the problems inherent in using relatively nonselective pharmacological inhibitors. In these experiments, lentiviral FAK.shRNA expression in *Nf2*$^{-/-}$ glia inhibited paxillin phosphorylation but had no effect on Src phosphorylation (Fig. 7B, upper panel). FAK shRNA inhibition in *Nf2*$^{-/-}$ glia also reduced the proliferation to levels observed in WT glia (Fig. 7B, lower panel). In addition, we inhibited paxillin expression in *Nf2*$^{-/-}$ glia with lentiviral Pxn.shRNA and observed no effect on either Src or FAK phosphorylation (Fig. 7C, upper panel); however, this reduced the proliferation of *Nf2*$^{-/-}$ glia to WT levels (Fig. 7C, lower panel). In both cases, no effects of FAK and paxillin inhibition on WT glial cell proliferation were observed. These experiments demonstrate that merlin negatively regulates glial cell proliferation in a Src-, FAK-, and paxillin-dependent manner

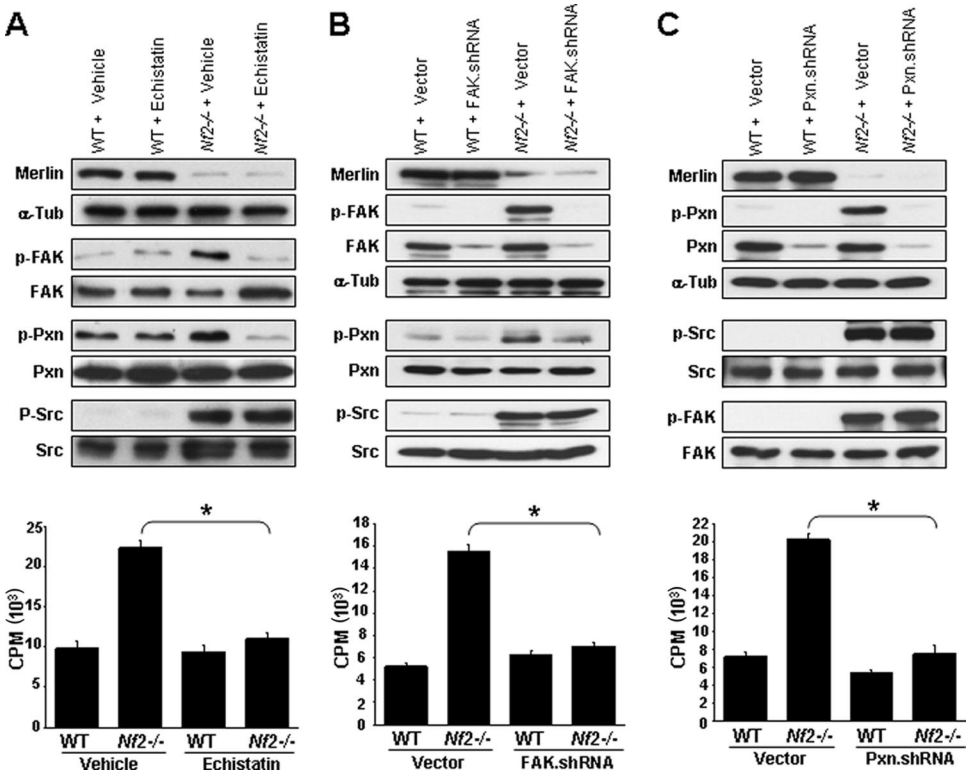

FIG. 7. Merlin growth regulation requires FAK and paxillin signaling. (A) (Top) Echistatin inhibits the phosphorylation of both FAK and paxillin but has no effect on Src activation. (Bottom) Echistatin treatment eliminates the growth advantage observed in $Nf2^{-/-}$ glia, as determined by [^{3}H]thymidine incorporation. *, $P < 0.001$ (unpaired t test). (B) (Top) FAK.shRNA inhibits the expression of FAK (>92% reduction) as well as the phosphorylation of both FAK and paxillin. No effect on Src activation was observed. (Bottom) FAK.shRNA treatment eliminates the growth advantage observed in $Nf2^{-/-}$ glia, as assessed by [^{3}H]thymidine incorporation. *, $P < 0.003$ (unpaired t test). (C) (Top) Pxn.shRNA treatment inhibits the expression of paxillin (>95% reduction) as well as the phosphorylation of paxillin but has no effect on FAK and Src activation. Total tubulin, Src, FAK, and paxillin expression levels were used as internal controls for equal protein loading. (Bottom) Pxn.shRNA treatment eliminates the growth advantage observed in $Nf2^{-/-}$ glia, as determined by [^{3}H]thymidine incorporation. *, $P < 0.001$ (unpaired t test).

and place paxillin downstream of Src and FAK in the merlin glial cell growth control pathway.

Merlin regulates glial cell proliferation through Src signaling in vivo. To demonstrate that merlin regulates glial cell proliferation in a Src-dependent manner in vivo, postnatal day 10 $Nf2^{GFAP}$CKO pups were injected with either the Src inhibitor PP2 or vehicle three times a week for 2 weeks (14). $Nf2^{GFAP}$CKO pups were then injected with BrdU, and the numbers of BrdU- and GFAP-positive glia were quantitated as previously reported (3, 24). Consistent with our findings in vitro, PP2 treatment of $Nf2^{GFAP}$CKO mice resulted in reductions in the numbers of BrdU (Fig. 8A)- and GFAP (Fig. 8B)-expressing cells to levels observed in $Nf2^{flox/flox}$ mice. Similarly, PP2 treatment decreased Src, FAK, and paxillin phosphorylation in $Nf2^{GFAP}$CKO mice to WT levels (Fig. 8C). PP2 treatment had no effect on glial cell numbers, proliferation, or Src pathway activity in $Nf2^{flox/flox}$ mice. Collectively, these results demonstrate that merlin also regulates glial cell growth in a Src-dependent manner in vivo.

Merlin regulates Src by modulating ErbB2 activation. Several receptor tyrosine kinase proteins have been shown to regulate Src activity, including ErbB2 (erythroblastic leukemia viral oncogene homolog 2) (36, 53) and EGFR (13, 19). Based on previous studies implicating EGFR in merlin growth regulation in non-nervous-system cells (9), we first examined EGFR in $Nf2^{-/-}$ glia in vitro and in $Nf2^{GFAP}$CKO mice in vivo. We found no changes in EGFR expression or phosphorylation in $Nf2^{-/-}$ glia relative to that in WT glia (Fig. 9A). Next, we examined the activation status of other members of the EGFR family, including ErbB2, ErbB3, and ErbB4, using phospho-specific antibodies. Whereas we observed no changes in ErbB3 or ErbB4 tyrosine phosphorylation (Fig. 9B), we observed a significant increase in ErbB2 phosphorylation on tyrosine 877 in $Nf2^{-/-}$ glial cells compared to that in WT glia (Fig. 9C). In contrast, no change in ErbB2 tyrosine 1248 phosphorylation was observed in $Nf2^{-/-}$ glial cells relative to that in WT glia (Fig. 9C). As expected, we also detected increased ErbB2 tyrosine 877 phosphorylation in $Nf2^{GFAP}$CKO compared to $Nf2^{flox/flox}$ mouse brains (Fig. 9D). To directly demonstrate that ErbB2 activity was increased in $Nf2^{-/-}$ glia, we assayed ErbB2 activity following ErbB2 immunoprecipitation. Similar to the results obtained with the ErbB2 Y877 phospho-antibody, we observed a 3.2-fold increase in ErbB2 activity in $Nf2^{-/-}$ glia relative to that in their WT counterparts (Fig. 9E). Lastly, to show that merlin is directly responsible for ErbB2 activation, we found that reexpression of WT but not L64P mutant merlin in $Nf2^{-/-}$ glia reduced ErbB2 Y877 phosphorylation to WT

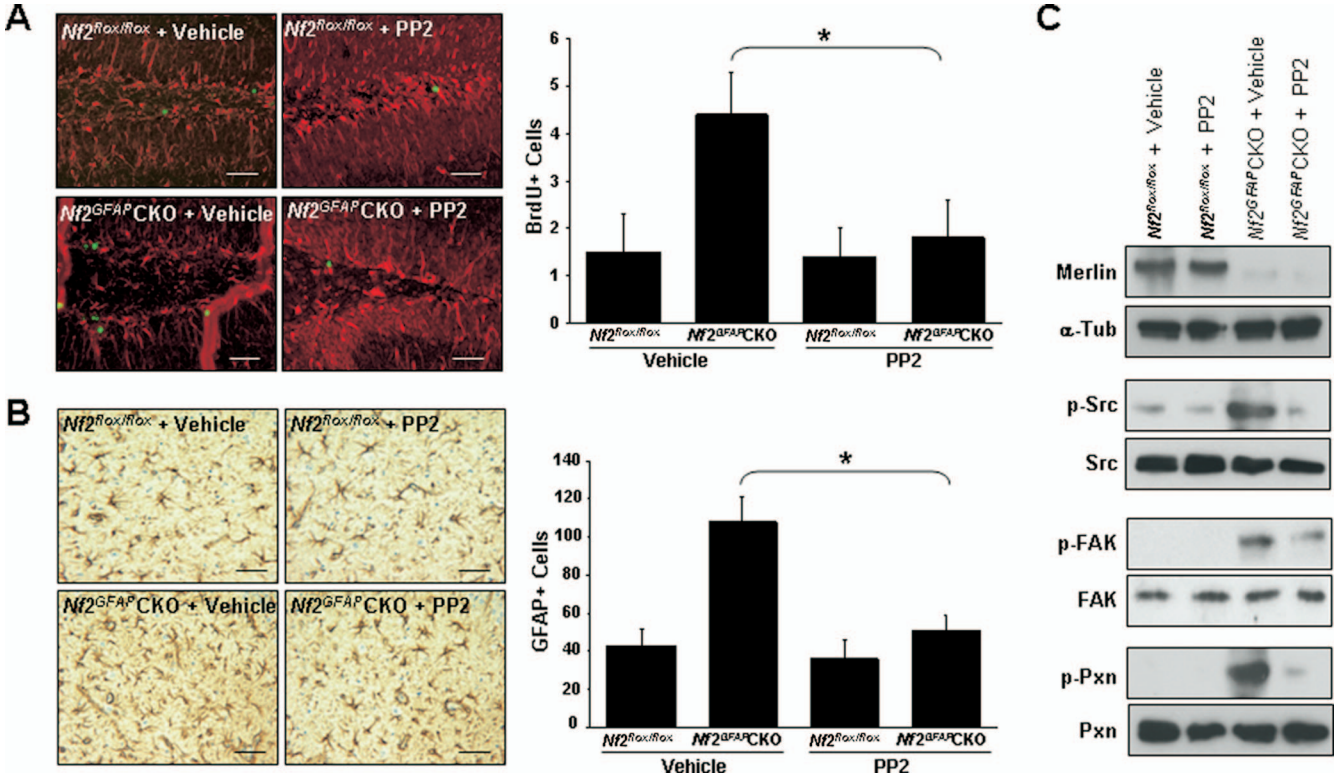

FIG. 8. Merlin regulation of glial cell growth is Src dependent in vivo. (A) Representative immunofluorescence photomicrographs of hippocampi from BrdU-injected $Nf2^{flox/flox}$ and $Nf2^{GFAP}$CKO mice, with or without treatment with the Src inhibitor PP2 (2 mg/kg). Images were labeled with both BrdU (green) and GFAP (red) antibodies. A twofold decrease in the number of BrdU-positive cells was observed in the PP2-treated $Nf2^{GFAP}$CKO brains compared to vehicle-treated mouse brains. *, $P = 0.001$ (unpaired t test). (B) Representative photomicrographs of hippocampi labeled with GFAP antibodies. PP2-treated $Nf2^{GFAP}$CKO mice exhibited a twofold decrease in the number of GFAP-labeled cells compared to vehicle-treated $Nf2^{GFAP}$CKO littermates. No effect of PP2 treatment on $Nf2^{flox/flox}$ mice was seen. *, $P < 0.002$ (unpaired t test). (C) Immunoblot analysis demonstrates amelioration of the increased Src, FAK, and paxillin activation following PP2 treatment. The expression levels of tubulin, total Src, FAK, and paxillin were used as internal controls for equal protein loading.

levels (Fig. 9F). No effect of merlin expression on ErbB2 Y877 phosphorylation was observed in WT glia.

Consistent with ErbB2 activation as the initiating signal in the merlin growth control pathway, inhibition of Src or Src effectors in vitro or in vivo had no effect on ErbB2 Y877 phosphorylation. In these studies, no changes in ErbB2 tyrosine 877 phosphorylation were seen following PP2 treatment of $Nf2^{-/-}$ glia in vitro (Fig. 10A, left panels), PP2 treatment of $Nf2^{GFAP}$CKO mouse brains in vivo (Fig. 10A, right panels), inhibition of FAK and paxillin by echistatin (Fig. 10B), or shRNA genetic inhibition of Src (Fig. 10C), FAK (Fig. 10D), and paxillin (Fig. 10E).

To determine whether merlin-dependent ErbB2 activation was responsible for Src-FAK-paxillin pathway activation as well as increased proliferation in $Nf2^{-/-}$ glia, we initially employed the ErbB2-specific inhibitor tyrphostin (AG825) (39). Following treatment of $Nf2^{-/-}$ glia with AG825, Src, FAK, and paxillin phosphorylation in $Nf2^{-/-}$ glial cells was reduced to WT levels (Fig. 11A, top panel). Similarly, ErbB2 inhibition also decreased $Nf2^{-/-}$ glial cell growth to the levels observed in WT glia (Fig. 11A, bottom panel). To provide additional evidence for the role of ErbB2 in merlin growth regulation, we employed ErbB2 silencing with lentiviral ErbB2.shRNA. In these experiments, loss of ErbB2 expression likewise reduced Src, FAK, and paxillin phosphorylation in $Nf2^{-/-}$ glia to WT levels (Fig. 11B, top panel). As observed following AG825 treatment, ErbB2 shRNA inhibition also decreased $Nf2^{-/-}$ glial cell growth to WT levels (Fig. 11B, bottom panel). These findings demonstrate that merlin selectively regulates ErbB2 activation, which is responsible for the increased Src signaling and proliferation observed in $Nf2^{-/-}$ glial cells.

Merlin regulates the interaction between Src and ErbB2. Based on the observation that ErbB2 can interact with both merlin (15) and Src (27, 36, 42), we next sought to determine whether merlin loss is associated with increased ErbB2-Src binding. In these experiments, ErbB2 was precipitated from WT and $Nf2^{-/-}$ glia using total ErbB2 antibodies. First, we confirmed that merlin binds to ErbB2 in WT glia and demonstrated that merlin loss in glia leads to a dramatic increase in both total and Y416-phosphorylated Src binding to ErbB2 (Fig. 12A). Second, we showed that the reintroduction of WT but not mutant merlin inhibited ErbB2-Src binding (Fig. 12B). Third, we found that inhibition of ErbB2 activation using the AG825 inhibitor blocked the interaction of ErbB2 with Src in $Nf2^{-/-}$ glia (Fig. 12C), whereas inhibition of Src activation with PP2 had no effect on ErbB2-Src binding (Fig. 12D). These findings demonstrate that only functional merlin can inhibit

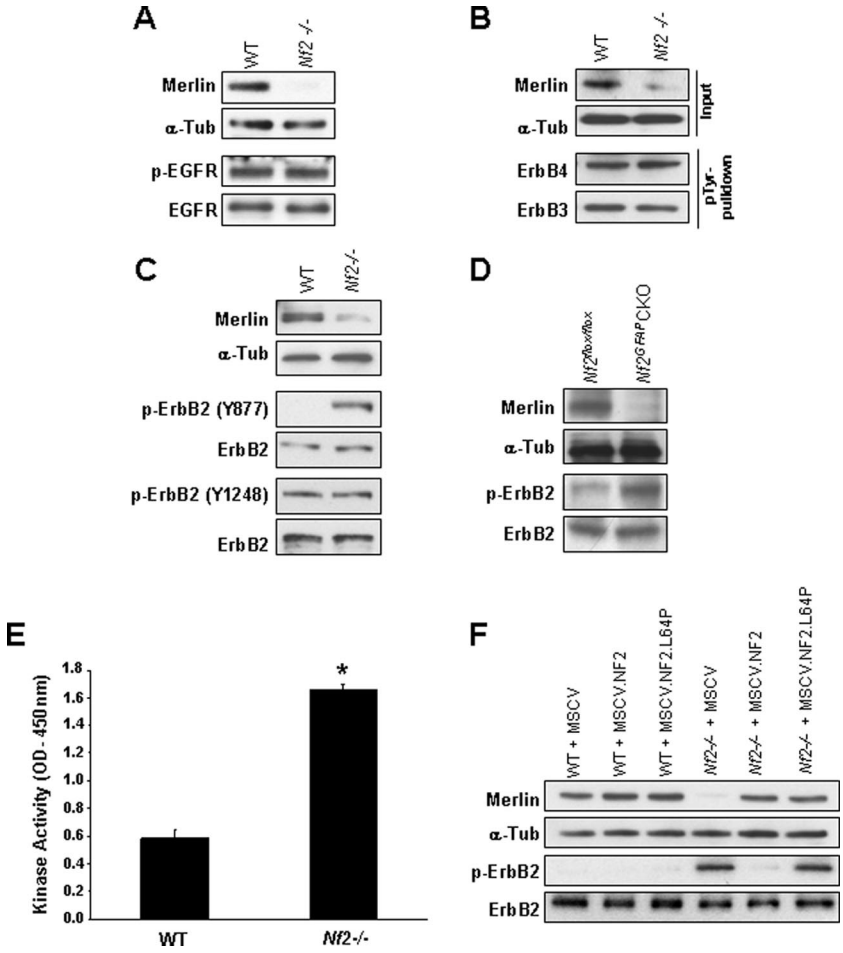

FIG. 9. Merlin regulates ErbB2 activation in glial cells. (A) Immunoblot analysis of WT and $Nf2^{-/-}$ glial lysates, using a phospho-specific EGFR antibody (Y845), demonstrates no change in EGFR activation. Total EGFR expression was used as an internal control for equal protein loading. (B) Immunoblot analyses of WT and $Nf2^{-/-}$ glial lysates following phosphotyrosine (pTyr) affinity binding with antibodies against ErbB4 and ErbB3 show no change in phosphorylation state for the other two ErbB family members. Merlin and tubulin expression levels were included as internal controls. (C) $Nf2^{-/-}$ glia exhibited a 7.2-fold increase in ErbB2-Y877 activation compared to WT controls in vitro, with no change in ErbB2-Y1248 phosphorylation. (D) $Nf2^{GFAP}$CKO mouse brains exhibited a 2.3-fold increase in ErbB2 (Y877) activation compared to WT controls in vivo, as assessed by immunoblotting analysis and scanning densitometry. (E) In an ErbB2 kinase activity assay, $Nf2^{-/-}$ glia exhibited a 3.2-fold increase in ErbB2 activity relative to WT glia. *, $P < 0.001$ (unpaired t test). OD, optical density. (F) WT but not mutant merlin expression reduces ErbB2 activation in $Nf2^{-/-}$ glia.

Src binding to ErbB2 and that the association between Src and ErbB2 is dependent on ErbB2 but not Src activity.

To determine whether ErbB2 binding to merlin and Src represents a direct interaction, we immunoprecipitated radiolabeled in vitro-transcribed/translated merlin and Src proteins with a recombinant ErbB2 protein containing the activation region of ErbB2 known to interact with Src (27). Both merlin and Src directly interacted with ErbB2 (Fig. 12E). Importantly, we observed no binding of mutant merlin (L64P) to ErbB2, consistent with its inability to restore normal growth regulation in $Nf2^{-/-}$ glia. We next sought to determine whether merlin and Src compete for binding to ErbB2. In these experiments, excess amounts of merlin or Src were added to interfere with Src-ErbB2 or merlin-ErbB2 binding, respectively. We show that merlin inhibited ErbB2-Src binding and Src inhibited ErbB2-merlin binding in a concentration-dependent manner (Fig. 12F and G).

To validate the Src-ErbB2 association results, we performed reciprocal immunoprecipitation studies, using Src to detect ErbB2 binding. In these experiments, we found that merlin loss in glia led to a dramatic increase in Src binding to ErbB2 (Fig. 13A) and that reexpression of WT but not mutant merlin inhibited ErbB2-Src binding (Fig. 13B). Moreover, the Src-ErbB2 interaction was dependent only on ErbB2 activation (Fig. 13C) and not Src activity (Fig. 13D). Interestingly, we also noticed that merlin was found in the Src immunoprecipitates from WT glial cells (Fig. 13A). However, unlike ErbB2-Src binding, the interaction between Src and merlin was not dependent on Src or ErbB2 activity.

The finding that merlin can associate with either Src or ErbB2 suggests two non-mutually exclusive models for merlin function. First, merlin may compete with Src for binding to ErbB2, such that merlin-ErbB2 binding precludes an association between Src and ErbB2. In this fashion, merlin loss allows Src to bind to ErbB2, which culminates in Src activation and increased glial cell growth. Second, merlin may bind to Src and

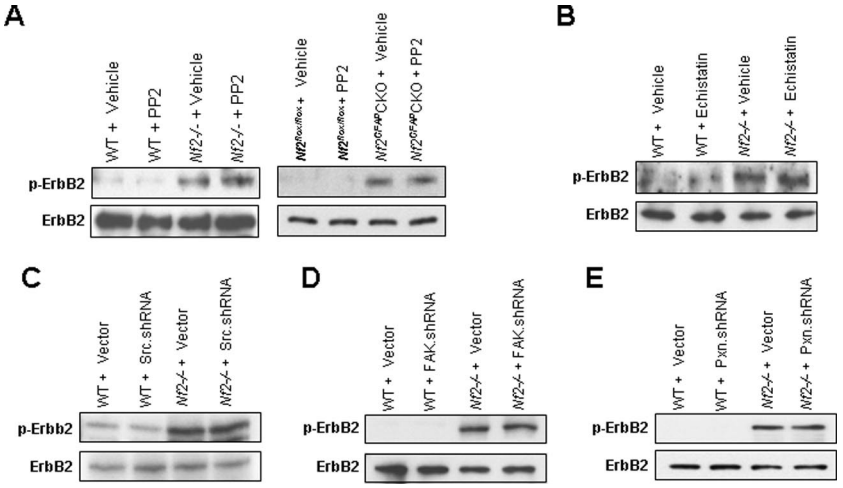

FIG. 10. ErbB2 activation functions upstream of Src/FAK/paxillin in the merlin glial control growth pathway. (A) PP2 treatment of $Nf2^{-/-}$ glial cells has no effect on ErbB2 hyperactivation in vitro or in vivo. (B) Echistatin treatment of $Nf2^{-/-}$ glial cells has no effect on ErbB2 hyperactivation in vitro. Genetic inhibition of Src (C), FAK (D), or paxillin (E) in $Nf2^{-/-}$ glial cells, using Src.shRNA, FAK.shRNA, or Pxn.shRNA, respectively, has no effect on ErbB2 hyperactivation. Total tubulin and total ErbB2 expression levels were used as internal loading controls.

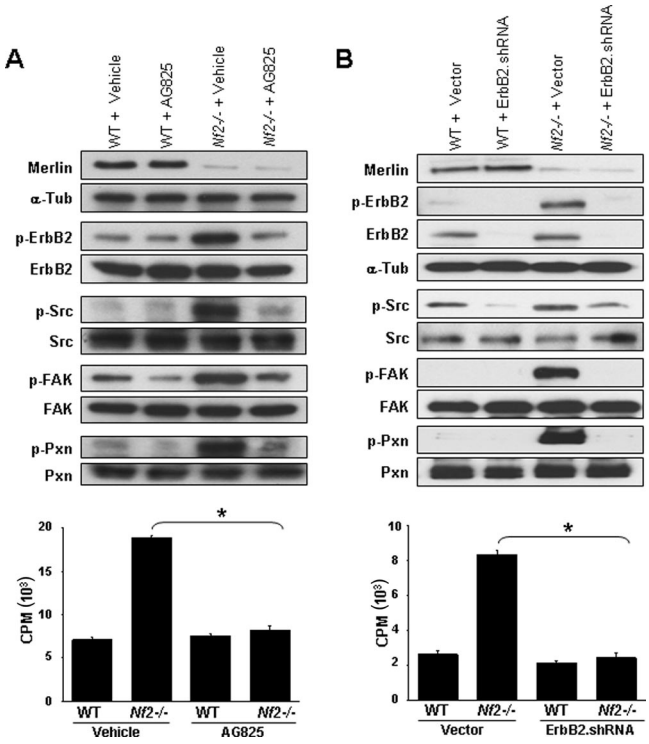

FIG. 11. Merlin regulation of glial cell growth requires ErbB2 activation. (A) (Top) Inhibition of ErbB2 activation with AG825 in $Nf2^{-/-}$ glia reduces Src, FAK, and paxillin hyperactivation to WT levels. (Bottom) AG825 treatment of $Nf2^{-/-}$ glia reduces cell proliferation to WT levels, as assessed by [^{3}H]thymidine incorporation. No effect of AG825 treatment was observed in WT glia. *, $P < 0.001$ (unpaired t test). (B) (Top) Inhibition of ErbB2 expression and activation with ErbB2.shRNA (>98% reduction) reduces the hyperactivation of Src, FAK, and paxillin in $Nf2^{-/-}$ glia to WT levels. Total tubulin, Src, FAK, and ErbB2 expression levels were used as internal loading controls. (Bottom) Treatment with ErbB2.shRNA but not with vector eliminates the growth advantage observed in $Nf2^{-/-}$ glia, as assessed by [^{3}H]thymidine incorporation. No effect of ErbB2.shRNA was observed in WT glia. *, $P < 0.002$ (unpaired t test).

sequester Src from binding to ErbB2. The loss of merlin would release Src to bind to ErbB2 and initiate Src-dependent signaling to increase glial cell proliferation.

To distinguish between these two possibilities, we sought to define the merlin residues important for Src and ErbB2 binding. In these experiments, we employed an in vitro binding assay using recombinant ErbB2 and Src proteins to determine which regions of merlin were necessary for merlin-ErbB2 and merlin-Src interactions. In vitro-transcribed/translated radiolabeled full-length merlin (WT) as well as merlin fragments containing residues 1 to 300 (NF2.N-term), 300 to 595 (NF2.C-term), and 300 to 557 were immunoprecipitated with recombinant ErbB2 or Src protein. Merlin binding to ErbB2 required C-terminal domain residues 300 to 557 (Fig. 14A), whereas merlin binding to Src required C-terminal domain residues 557 to 595 (Fig. 14B). These findings demonstrate that the residues important for merlin binding to Src and ErbB2 are distinct and separable.

Since the merlin C-terminal fragment containing residues 300 to 557 binds only to ErbB2 and not to Src, we took advantage of this selective binding to discriminate between the two possible models of merlin function. We found that increasing amounts of the merlin C-terminal 300-557 fragment inhibited Src binding to ErbB2 (Fig. 14C). In contrast, increasing amounts of Src did not inhibit the association between the merlin C-terminal 300-557 fragment and ErbB2 (Fig. 14D). These results indicate that merlin binding to ErbB2 precludes the ability of Src to associate with ErbB2 and that the association between merlin and ErbB2 likely interferes with ErbB2-mediated activation of Src.

DISCUSSION

In this report, we use GFAP-positive (glial) cells in vitro and in vivo as a model system to define the mechanism underlying merlin growth regulation in the CNS. First, we show that *Nf2*-deficient glia exhibit increased proliferation, which is reversed by merlin reexpression. Second, we demonstrate that merlin

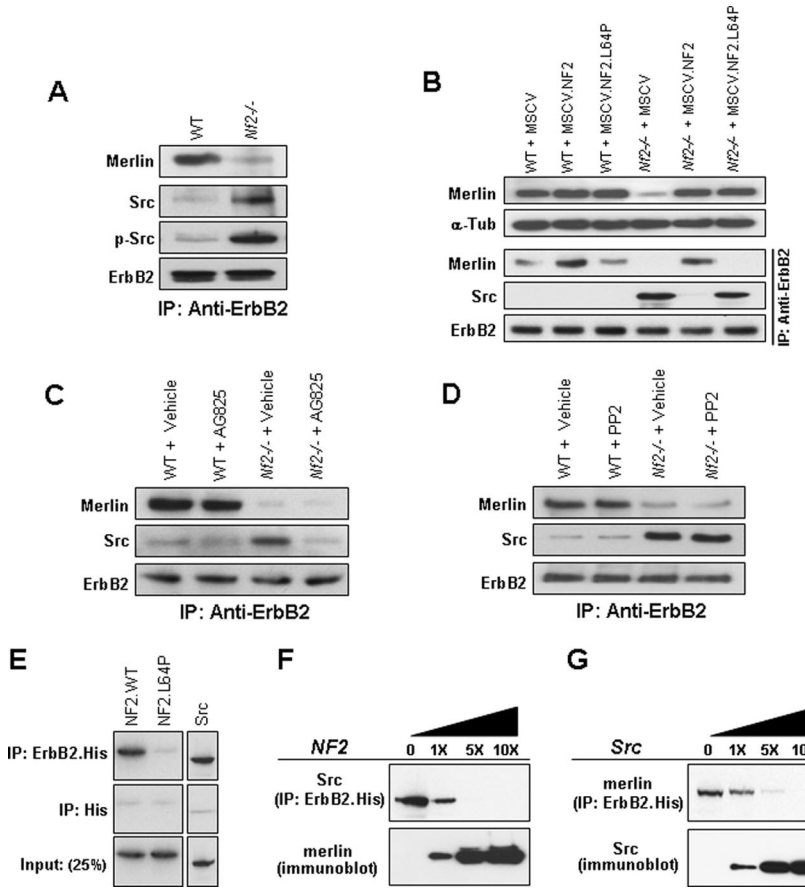

FIG. 12. Merlin directly regulates the interaction between ErbB2 and Src. (A) Immunoprecipitation of ErbB2 from WT and $Nf2^{-/-}$ glia shows that the association between ErbB2 and Src as well as ErbB2 and p-Src (Y416) occurs only in *Nf2*-deficient glia. (B) WT but not mutant merlin expression inhibits ErbB2 and Src interaction in $Nf2^{-/-}$ glia. (C) AG825 treatment inhibits the association between ErbB2 and Src in *Nf2*-deficient glia. (D) PP2 treatment has no effect on the association between ErbB2 and Src in *Nf2*-deficient glia. Total ErbB2 was used as an internal control for ErbB2 precipitation. (E) Src and merlin directly associate with ErbB2 following immunoprecipitation of [^{35}S]methionine-radiolabeled merlin (NF2.WT or NF2.L64P) or Src proteins with recombinant His-tagged ErbB2 (ErbB2.His). (Top) No binding to ErbB2 was observed with mutant merlin. (Middle) In the absence of the ErbB2 recombinant protein, there was no binding of radiolabeled NF2.WT, NF2.L64P, or Src protein to the His affinity gel. (Bottom) Input levels of radiolabeled NF2.WT, NF2.L64P, and Src proteins in the ErbB2.His immunoprecipitation analysis were used as normalization controls in scanning densitometric analyses to determine the percentages of bound proteins. A total of 32% of radiolabeled NF2.WT and 28% of Src proteins were bound to recombinant ErbB2 protein, whereas <1% of NF2.L64P was bound to ErbB2. (F) (Top) ErbB2-Src binding was decreased 67% in the presence of equal amounts of merlin and completely eliminated in the presence of a fivefold excess of merlin. (G) (Top) ErbB2-merlin binding was decreased 52% in the presence of equal amounts of Src, decreased 94% in the presence of a 5-fold excess of Src, and completely eliminated in the presence of a 10-fold excess of Src (top). (Bottom [F and G]) Immunoblotting was used to verify the amounts of nonradiolabeled merlin and Src added to each reaction mix.

regulation of glial cell growth requires ErbB2 activation, ErbB2-Src binding, and Src pathway activity in vitro and in vivo. Third, based on the direct binding of merlin to Src and ErbB2, we propose a molecular mechanism for merlin function in glia in which merlin competitively inhibits the association between Src and ErbB2. Importantly, although no visible tumors were observed in our *Nf2* glial conditional knockout mice, these results identify a critical targetable growth control pathway in glia relevant to human NF2-associated glial cell tumors.

The lack of glial tumors in the *Nf2* glial conditional knockout mice may reflect the generally low incidence of tumor formation in *Nf2* conditional knockout GEM strains. In this regard, the incidence of nervous system tumor formation in the schwannoma and meningioma *Nf2* GEM models ranged between 24% and 29%, with an average latency of 10 to 14 months (18, 26). While we aged the $Nf2^{GFAP}$CKO mice for 15 months and performed detailed necropsies, it is possible that tumor formation will require larger numbers of mice and longer periods of observation. Alternatively, it is possible that glial cell tumor formation requires stromal *Nf2* heterozygosity, as we have previously reported for NF1-associated optic gliomas in *Nf1* optic glioma GEM models (2, 3, 64). Future experiments are necessary to explore these possibilities.

Previous studies with other cell types have shown that Src controls cell proliferation and motility by signaling through downstream effectors, including FAK and paxillin (8). In $Nf2^{-/-}$ glia, we found that Src hyperactivation leads to the sequential activation/phosphorylation of FAK and paxillin and that Src, FAK, and paxillin are responsible for the increased

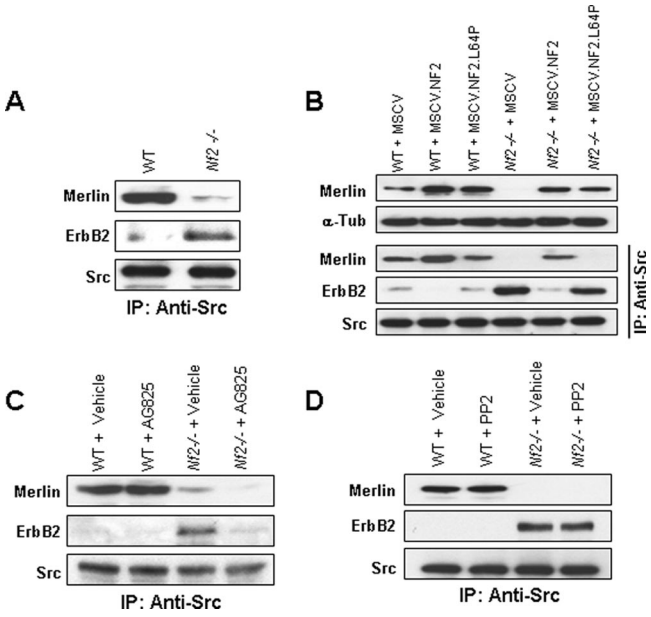

FIG. 13. Merlin interacts with both ErbB2 and Src. (A) Immunoprecipitation of Src from WT and $Nf2^{-/-}$ glia shows that the association between Src and ErbB2 occurs only in *Nf2*-deficient glia. (B) WT but not mutant merlin expression inhibits Src and ErbB2 interaction in $Nf2^{-/-}$ glia. (C) AG825 treatment inhibits the association between Src and ErbB2 in *Nf2*-deficient glia. (D) PP2 treatment has no effect on the association between Src and ErbB2 in *Nf2*-deficient glia. Total Src was used as an internal control for Src precipitations. In WT glia, merlin and Src associate; however, this binding is not affected by SrbB2 or Src activation.

proliferation observed in *Nf2*-deficient glia in vitro and in vivo. These findings are compatible with prior reports demonstrating that FAK and paxillin colocalize and physically associate with merlin (15, 57). In addition, merlin reexpression in *NF2*-deficient malignant mesothelioma cells has been found to attenuate FAK phosphorylation and to inhibit the interaction between FAK and Src (41). While the exact mechanism underlying FAK growth regulation has not been elucidated fully, recent evidence suggests that FAK may control cell growth by suppressing p21 and p27 cyclin-dependent kinase inhibitor levels (6, 12). However, in preliminary experiments, we detected no changes in p21 and p27 expression in $Nf2^{-/-}$ glia relative to WT glia (S. S. Houshmandi and D. H. Gutmann, unpublished observations).

Our finding that paxillin is required for merlin growth control in glial cells is consistent with previous reports demonstrating that paxillin can regulate cell proliferation in other cell types (22, 56). While the mechanism of paxillin growth regulation is not clear, paxillin may control cell growth by modulating the expression or activation of select transcription factors, such as AP-1 and c-Jun (56). We examined the expression of these transcription factors, as well as others implicated in growth control, by using RNA microarray profiling of WT and $Nf2^{-/-}$ glia and found no changes in the expression of relevant transcription factors (Houshmandi and Gutmann, unpublished observations). Studies are ongoing in our laboratory to determine the precise manner by which FAK and paxillin regulate cell growth in CNS glia.

Src has been implicated in the control of many intracellular signaling pathways, initiated by cell surface receptor activation, which regulate cell differentiation, survival, proliferation, and motility (58). Previous studies have shown that the growth regulatory function of merlin may be mediated in a variety of different cell types by its interaction with several cell surface receptors, including CD44, β1-integrin, ErbB2, and EGFR (9, 15, 35, 38). While all of these receptors have been shown to regulate Src activity in other cell types, only ErbB2 has been shown to form complexes with CD44, EGFR, and β1-integrin. In this regard, ErbB2 represents a logical candidate for a cell surface receptor capable of integrating multiple environmental signals relevant to merlin growth regulation. In this report, we demonstrate for the first time that ErbB2 plays a critical role in regulating Src-mediated proliferation in $Nf2^{-/-}$ glia and that ErbB2 is the main ErbB receptor kinase family member whose activation is deregulated by merlin loss in glial cells.

Consistent with the role of ErbB2 in controlling cell differentiation, survival, and growth, ErbB2 has been shown to interact with several molecules previously implicated in merlin growth regulation in other cell types, including CD44. In this regard, ErbB2 interacts with CD44 in ovarian carcinoma cell lines and has been shown to regulate ovarian carcinoma cell growth (63). In addition, ErbB2 also interacts with EGFR to regulate glioma cell proliferation (28, 40) and motility (41). In the present study, we show that ErbB2 is hyperactivated in *Nf2*-deficient glia in vitro and in vivo and that pharmacologic or genetic inhibition of ErbB2 in vitro reverses the growth phenotype seen in $Nf2^{-/-}$ glia. While the exact mechanism underlying merlin regulation of ErbB2 activation is not known, these findings raise the intriguing possibility that ErbB2 is a central mediator of cell signaling and might integrate growth regulatory messages from other cell membrane receptors. In the absence of merlin, these receptor associations may not form, leading to deregulated ErbB2 activation. In support of this mechanism, preliminary studies in our laboratory have recently shown that the interactions between ErbB2 and CD44, ErbB2 and EGFR, and ErbB2 and another ErbB2 binding partner, ErbB4, are all dramatically attenuated in $Nf2^{-/-}$ glia (Houshmandi and Gutmann, unpublished observations).

Finally, we show that merlin regulates ErbB2-mediated activation of Src. This observation is consistent with previous studies which have shown that ErbB2 interacts with and activates Src in breast cancer cells and that ErbB2-Src binding is specific to the catalytic domain of ErbB2 (27, 36). In $Nf2^{-/-}$ glia, we found increased ErbB2-Src binding, which was blocked by pharmacologic ErbB2 inhibition. It is worth noting that the increase in Src and ErbB2 phosphorylation in *Nf2*-deficient glia is limited to specific sites in the catalytic domain of each protein (Src-Y416 and ErbB2-Y877) which have been predicted to regulate their activation and to mediate their interactions with other proteins (27). In this report, we demonstrate that a recombinant ErbB2 cytoplasmic domain protein which contains the activation region as well as the Src-interacting domain directly interacts with merlin and Src in vitro and that merlin competitively inhibits the interaction between Src and ErbB2 in a concentration-dependent manner. We further show that merlin binding to ErbB2 and Src involves different residues in the C terminus of the merlin protein. We took advan-

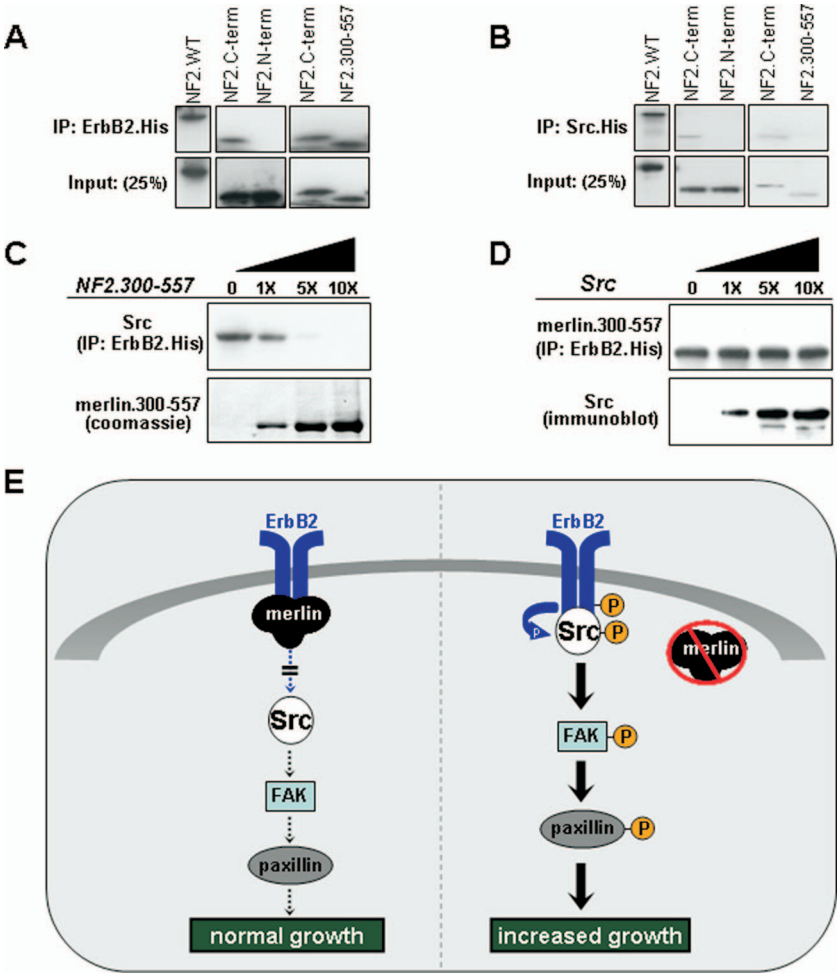

FIG. 14. Merlin binding to ErbB2 precludes the association of Src with ErbB2. (A) In an in vitro binding assay, [^{35}S]methionine-radiolabeled full-length merlin containing residues 1 to 595 (NF2.WT), NF2.C-term containing residues 300 to 595, and NF2.C-term containing residues 300 to 557, bound to recombinant His-tagged ErbB2 (ErbB2.His). In contrast, no binding to ErbB2 was observed using NF2.N-term containing residues 1 to 300. Input levels for the reactions are shown and were used as normalization controls in scanning densitometric analyses to determine the percentages of bound proteins. Thirty percent of radiolabeled NF2.WT, 25% of NF2.C-term, and 24% of NF2.300-557 bound to recombinant ErbB2 protein, whereas <1% of NF2.N-term bound to ErbB2. (B) In an in vitro binding assay, [^{35}S]methionine-radiolabeled full-length merlin containing residues 1 to 595 (NF2.WT), and NF2.C-term containing residues 300 to 595, bound to recombinant His-tagged ErbB2 (ErbB2.His). In contrast, no binding to ErbB2 was observed using either NF2.C-term containing residues 300 to 557, or NF2.N-term containing residues 1 to 300. Input levels for the reactions are shown and were used as normalization controls in scanning densitometric analyses to determine the percentages of bound proteins. Thirty-one percent of radiolabeled NF2.WT and 19% of NF2.C-term bound to recombinant Src protein, whereas <1% of NF2.N-term and NF2.300-557 bound to Src. (C) (Top) ErbB2-Src binding was decreased 48% in the presence of equal amounts of NF2.300-557, decreased 96% in the presence of a 5-fold excess of NF2.300-557, and completely eliminated in the presence of a 10-fold excess of NF2.300-557. (Bottom) Coomassie staining was used to verify the amount of nonradiolabeled NF2.300-557 added to each reaction mix. (D) (Top) NF2.300-557–ErbB2 binding was not altered by equal or excess amounts of Src. (Bottom) Immunoblotting was used to verify the amount of nonradiolabeled Src added to the reaction mixtures. (E) Potential molecular model for merlin growth regulation in glial cells. In WT cells, merlin associates with ErbB2 and precludes Src binding to ErbB2. In the absence of functional merlin, Src binds to activated ErbB2, leading to ErbB2-mediated Src phosphorylation/activation, Src effector protein phosphorylation, and increased glial cell growth.

tage of this differential merlin binding to demonstrate that merlin binding to ErbB2 blocks Src binding. Based on these findings, we propose a novel mechanism for merlin function (Fig. 14E). In WT cells, merlin binds to the cytoplasmic domain of ErbB2 and precludes an association between Src and ErbB2. However, in the absence of merlin, Src binds to activated ErbB2, which results in increased Src activity, Src effector activation, and increased cell growth. Our results demonstrating a central role for ErbB2 and Src in regulating *NF2*-deficient glial cell growth suggest that potential therapeutic approaches for treating NF2-associated tumors might involve targeting ErbB2 and/or Src activation. With the recent success employing ErbB2 inhibitors (e.g., trastuzumab) and Src kinase inhibitors (e.g., dasatinib) in clinical studies for the treatment of breast cancer (40, 43) and myelogenous leukemia (16, 31, 37), the future use of these and related inhibitors may prove beneficial for the treatment of human tumors characterized by merlin loss of function.

ACKNOWLEDGMENTS

This work was supported in part by Department of Defense grant DAMD17-04-0266 (to D.H.G.), with a nested postdoctoral fellowship (S.S.H.). We also acknowledge the generous support of the Vincent Buono Research Fund (to D.H.G. Hand M.G.).

Additionally, we thank Ron Bose, Sutapa Banerjee, Nicole Hicklin, Scott Gianino, and Cory Lewis for their technical assistance during the preparation of the manuscript.

REFERENCES

1. **Bai, Y., Y. J. Liu, H. Wang, Y. Xu, I. Stamenkovic, and Q. Yu.** 2006. Inhibition of the hyaluronan-CD44 interaction by merlin contributes to the tumor-suppressor activity of merlin. Oncogene **26:**836–850.
2. **Bajenaru, M. L., M. R. Hernandez, A. Perry, Y. Zhu, L. F. Parada, J. R. Garbow, and D. H. Gutmann.** 2003. Optic nerve glioma in mice requires astrocyte Nf1 gene inactivation and Nf1 brain heterozygosity. Cancer Res. **63:**8573–8577.
3. **Bajenaru, M. L., Y. Zhu, N. M. Hedrick, J. Donahoe, L. F. Parada, and D. H. Gutmann.** 2002. Astrocyte-specific inactivation of the neurofibromatosis 1 gene (NF1) is insufficient for astrocytoma formation. Mol. Cell. Biol. **22:** 5100–5113.
4. **Bourn, D., G. Evans, S. Mason, S. Tekes, L. Trueman, and T. Strachan.** 1995. Eleven novel mutations in the NF2 tumour suppressor gene. Hum. Genet. **95:**572–574.
5. **Bretscher, A., K. Edwards, and R. Fehon.** 2002. ERM proteins and merlin: integrators at the cell cortex. Nat. Rev. Mol. Cell Biol. **3:**586–599.
6. **Bryant, P., Q. Zheng, and K. Pumiglia.** 2006. Focal adhesion kinase controls cellular levels of p27/Kip1 and p21/Cip1 through Skp2-dependent and -independent mechanisms. Mol. Cell. Biol. **26:**4201–4213.
7. **Chadee, D. N., D. Xu, G. Hung, A. Andalibi, D. J. Lim, Z. Luo, D. H. Gutmann, and J. M. Kyriakis.** 2006. Mixed-lineage kinase 3 regulates B-Raf through maintenance of the B-Raf/Raf-1 complex and inhibition by the NF2 tumor suppressor protein. Proc. Natl. Acad. Sci. USA **103:**4463–4468.
8. **Cox, B. D., M. Natarajan, M. R. Stettner, and C. L. Gladson.** 2006. New concepts regarding focal adhesion kinase promotion of cell migration and proliferation. J. Cell Biochem. **99:**35–52.
9. **Curto, M., B. K. Cole, D. Lallemand, C. H. Liu, and A. I. McClatchey.** 2007. Contact-dependent inhibition of EGFR signaling by Nf2/Merlin. J. Cell Biol. **177:**893–903.
10. **Dasgupta, B., W. Li, A. Perry, and D. H. Gutmann.** 2005. Glioma formation in neurofibromatosis 1 reflects preferential activation of K-RAS in astrocytes. Cancer Res. **65:**236–245.
11. **Della Morte, R., C. Squillacioti, C. Garbi, P. Derkinderen, M. A. Belisario, J. A. Girault, P. Di Natale, L. Nitsch, and N. Staiano.** 2000. Echistatin inhibits pp125FAK autophosphorylation, paxillin phosphorylation and pp125FAK-paxillin interaction in fibronectin-adherent melanoma cells. Eur. J. Biochem. **267:**5047–5054.
12. **Ding, Q., J. R. Grammer, M. A. Nelson, J. L. Guan, J. E. Stewart, Jr., and C. L. Gladson.** 2005. p27Kip1 and cyclin D1 are necessary for focal adhesion kinase regulation of cell cycle progression in glioblastoma cells propagated in vitro and in vivo in the scid mouse brain. J. Biol. Chem. **280:**6802–6815.
13. **Dise, R. S., M. R. Frey, R. H. Whitehead, and D. B. Polk.** 2008. Epidermal growth factor stimulates RAC activation through SRC and phosphatidylinositol 3-kinase to promote colonic epithelial cell migration. Am. J. Physiol. Gastrointest. Liver Physiol. **294:**G276–G285.
14. **Duxbury, M. S., H. Ito, M. J. Zinner, S. W. Ashley, and E. E. Whang.** 2004. Inhibition of SRC tyrosine kinase impairs inherent and acquired gemcitabine resistance in human pancreatic adenocarcinoma cells. Clin. Cancer Res. **10:**2307–2318.
15. **Fernandez-Valle, C., Y. Tang, J. Ricard, A. Rodenas-Ruano, A. Taylor, E. Hackler, J. Biggerstaff, and J. Iacovelli.** 2002. Paxillin binds schwannomin and regulates its density-dependent localization and effect on cell morphology. Nat. Genet. **31:**354–362.
16. **Finn, R. S., J. Dering, C. Ginther, C. A. Wilson, P. Glaspy, N. Tchekmedyian, and D. J. Slamon.** 2007. Dasatinib, an orally active small molecule inhibitor of both the Src and Abl kinases, selectively inhibits growth of basal-type/"triple-negative" breast cancer cell lines growing in vitro. Breast Cancer Res. Treat. **105:**319–326.
17. **Gerber, M. A., S. M. Bahr, and D. H. Gutmann.** 2006. Protein 4.1B/differentially expressed in adenocarcinoma of the lung-1 functions as a growth suppressor in meningioma cells by activating Rac1-dependent c-Jun-NH(2)-kinase signaling. Cancer Res. **66:**5295–5303.
18. **Giovannini, M., E. Robanus-Maandag, M. van der Valk, M. Niwa-Kawakita, V. Abramowski, L. Goutebroze, J. M. Woodruff, A. Berns, and G. Thomas.** 2000. Conditional biallelic Nf2 mutation in the mouse promotes manifestations of human neurofibromatosis type 2. Genes Dev. **14:**1617–1630.
19. **Goi, T., M. Shipitsin, Z. Lu, D. A. Foster, S. G. Klinz, and L. A. Feig.** 2000. An EGF receptor/Ral-GTPase signaling cascade regulates c-Src activity and substrate specificity. EMBO J. **19:**623–630.
20. **Gutmann, D. H., R. T. Geist, H. Xu, J. S. Kim, and S. Saporito-Irwin.** 1998. Defects in neurofibromatosis 2 protein function can arise at multiple levels. Hum. Mol. Genet. **7:**335–345.
21. **Gutmann, D. H., M. J. Giordano, A. S. Fishback, and A. Guha.** 1997. Loss of merlin expression in sporadic meningiomas, ependymomas and schwannomas. Neurology **49:**267–270.
22. **Hamamura, K., K. Furukawa, T. Hayashi, T. Hattori, J. Nakano, H. Nakashima, T. Okuda, H. Mizutani, H. Hattori, M. Ueda, T. Urano, K. O. Llyod, and K. Furukawa.** 2005. Ganglioside GD3 promotes cell growth and invasion through p130Cas and paxillin in malignant melanoma cells. Proc. Natl. Acad. Sci. USA **102:**11041–11046.
23. **Hanke, J. H., J. P. Gardner, R. L. Dow, P. S. Changelian, W. H. Brissette, E. J. Weringer, B. A. Pollok, and P. A. Connelly.** 1996. Discovery of a novel, potent, and Src family-selective tyrosine kinase inhibitor. Study of Lck- and FynT-dependent T cell activation. J. Biol. Chem. **271:**695–701.
24. **Houshmandi, S. S., E. I. Surace, H. B. Zhang, G. N. Fuller, and D. H. Gutmann.** 2006. Tumor suppressor in lung cancer-1 (TSLC1) functions as a glioma tumor suppressor. Neurology **67:**1863–1866.
25. **Jin, H., T. Sperka, P. Herrlich, and H. Morrison.** 2006. Tumorigenic transformation by CPI-17 through inhibition of a merlin phosphatase. Nature **442:**576–579.
26. **Kalamarides, M., M. Niwa-Kawakita, H. Leblois, V. Abramowski, M. Perricaudet, A. Janin, G. Thomas, D. H. Gutmann, and M. Giovannini.** 2002. Nf2 gene inactivation in arachnoidal cells is rate-limiting for meningioma development in the mouse. Genes Dev. **16:**1060–1065.
27. **Kim, H., R. Chan, D. L. Dankort, D. Zuo, M. Najoukas, M. Park, and W. J. Muller.** 2005. The c-Src tyrosine kinase associates with the catalytic domain of ErbB-2: implications for ErbB-2 mediated signaling and transformation. Oncogene **24:**7599–7607.
28. **Lallemand, D., M. Curto, I. Saotome, M. Giovannini, and A. I. McClatchey.** 2003. NF2 deficiency promotes tumorigenesis and metastasis by destabilizing adherens junctions. Genes Dev. **17:**1090–1100.
29. **Lekanne Deprez, R. H., A. B. Bianchi, N. A. Groen, D. R. Seizinger, A. Hagmeijer, E. van Drunen, D. Bootsma, J. Koper, C. Avezaat, and N. Kley.** 1994. Frequent NF2 gene transcript mutations in sporadic meningiomas and vestibular schwannomas. Am. J. Hum. Genet. **54:**1022–1029.
30. **Lim, J. Y., H. Kim, S. S. Jeun, S. G. Kang, and K. J. Lee.** 2006. Merlin inhibits growth hormone-regulated Raf-ERKs pathways by binding to Grb2 protein. Biochem. Biophys. Res. Commun. **340:**1151–1157.
31. **Lombardo, L. J., F. Y. Lee, P. Chen, D. Norris, J. C. Barrish, K. Behnia, S. Castaneda, L. A. Cornelius, J. Das, A. M. Doweyko, C. Fairchild, J. T. Hunt, I. Inigo, K. Johnston, A. Kamath, D. Kan, H. Klei, P. Marathe, S. Pang, R. Peterson, S. Pitt, G. L. Schieven, R. J. Schmidt, J. Tokarski, M. L. Wen, J. Wityak, and R. M. Borzilleri.** 2004. Discovery of *N*-(2-chloro-6-methyl-phenyl)-2-(6-(4-(2-hydroxyethyl)-piperazin-1-yl)-2-methylpyrimidin-4-ylamino)thiazole-5-carboxamide (BMS-354825), a dual Src/Abl kinase inhibitor with potent antitumor activity in preclinical assays. J. Med. Chem. **47:**6658–6661.
32. **Louvet-Vallee, S.** 2000. ERM proteins: from cellular architecture to cell signaling. Biol. Cell. **92:**305–316.
33. **Mérel, P., K. Hoang-Xuan, M. Sanson, A. Moreau-Aubry, E. K. Bijlsma, C. Lazaro, J. P. Moisan, F. Resche, I. Nishisho, X. Estivill, J. Y. Delattre, M. Poisson, T. Hulsebos, O. Delattre, and G. Thomas.** 1995. Predominant occurrence of somatic mutations of the NF2 gene in meningiomas and schwannomas. Genes Chromosomes Cancer **13:**211–216.
34. **Morrison, H., T. Sperka, J. Manent, M. Giovannini, H. Ponta, and P. Herrlich.** 2007. Merlin/neurofibromatosis type 2 suppresses growth by inhibiting the activation of Ras and Rac. Cancer Res. **67:**520–527.
35. **Morrison, H., L. S. Sherman, J. Legg, F. Banine, C. Isacke, C. A. Haipek, D. H. Gutmann, H. Ponta, and P. Herrlich.** 2001. The NF2 tumor suppressor gene product, merlin, mediates contact inhibition of growth through interactions with CD44. Genes Dev. **15:**968–980.
36. **Muthuswamy, S. K., and W. J. Muller.** 1995. Direct and specific interaction of c-Src with Neu is involved in signaling by the epidermal growth factor receptor. Oncogene **11:**271–279.
37. **Nam, S., D. Kim, J. Q. Cheng, S. Zhang, D. J. Lee, R. Buettner, J. Mirosevich, F. Y. Lee, and R. Jove.** 2005. Action of the Src family kinase inhibitor, dasatinib (BMS-354825), on human prostate cancer cells. Cancer Res. **65:** 9185–9189.
38. **Obremski, V. J., A. M. Hall, and C. Fernandez-Valle.** 1998. Merlin, the neurofibromatosis type 2 gene product, and beta1 integrin associate in isolated and differentiating Schwann cells. J. Neurobiol. **37:**487–501.
39. **Osherov, N., A. Gazit, C. Gilon, and A. Levitzki.** 1993. Selective inhibition of the epidermal growth factor and HER2/neu receptors by tyrphostins. J. Biol. Chem. **268:**11134–11142.
40. **Piccart-Gebhart, M. J., M. Procter, B. Leyland-Jones, A. Goldhirsch, M. Untch, I. Smith, L. Gianni, J. Baselga, R. Bell, C. Jackisch, D. Cameron, M. Dowsett, C. H. Barrios, G. Steger, C. S. Huang, M. Andersson, M. Inbar, M. Lichinitser, I. Láng, U. Nitz, H. Iwata, C. Thomssen, C. Lohrisch, T. M. Suter, J. Rüschoff, T. Suto, V. Greatorex, C. Ward, C. Straehle, E. McFadden, M. S. Dolci, R. D. Gelber, and Herceptin Adjuvant (HERA) Trial Study Team.** 2005. Trastuzumab after adjuvant chemotherapy in HER2-positive breast cancer. N. Engl. J. Med. **353:**1659–1672.
41. **Poulikakos, P. I., G. H. Xiao, R. Gallagher, S. Jablonski, S. C. Jhanwar, and**

J. R. Testa. 2006. Re-expression of the tumor suppressor NF2/merlin inhibits invasiveness in mesothelioma cells and negatively regulates FAK. Oncogene **25:**5960–5968.
42. **Ren, Z., and T. S. Schaefer.** 2002. ErbB-2 activates Stat3 alpha in a Src- and JAK2-dependent manner. J. Biol. Chem. **277:**38486–38493.
43. **Romond, E. H., E. A. Perez, J. Bryant, V. J. Suman, C. E. Geyer, Jr., N. E. Davidson, E. Tan-Chiu, S. Martino, S. Paik, P. A. Kaufman, S. M. Swain, T. M. Pisansky, L. Fehrenbacher, L. A. Kutteh, V. G. Vogel, D. W. Visscher, G. Yothers, R. B. Jenkins, A. M. Brown, S. R. Dakhil, E. P. Mamounas, W. L. Lingle, P. M. Klein, J. N. Ingle, and N. Wolmark.** 2005. Trastuzumab plus adjuvant chemotherapy for operable HER2-positive breast cancer. N. Engl. J. Med. **353:**1673–1684.
44. **Rong, R., X. Tang, D. H. Gutmann, and K. Ye.** 2004. Neurofibromatosis 2 (NF2) tumor suppressor merlin inhibits phosphatidylinositol 3-kinase through binding to PIKE-L. Proc. Natl. Acad. Sci. USA **101:**18200–18205.
45. **Roskoski, R., Jr.** 2005. Src kinase regulation by phosphorylation and dephosphorylation. Biochem. Biophys. Res. Commun. **331:**1–14.
46. **Rouleau, G. A., P. Merel, M. Lutchman, M. Sanson, J. Zucman, C. Marineau, K. Hoang-Xuan, S. Demczuk, C. Desmaze, B. Plougastel, S. M. Pulst, G. Lenoir, E. Bijlsma, R. Fashold, J. Dumanski, P. De Jong, D. Parry, R. Eldrige, A. Aurias, O. Delattre, and G. Thomas.** 1993. Alteration in a new gene encoding a putative membrane-organizing protein causes neuro-fibromatosis type 2. Nature **10:**515–521.
47. **Ruttledge, M. H., J. Sarrazin, S. Rangaratnam, C. M. Phelan, E. Twist, P. Merel, O. Delattre, G. Thomas, M. Nordenskjöld, and V. P. Collins.** 1994. Evidence for the complete inactivation of the NF2 gene in the majority of sporadic meningiomas. Nat. Genet. **6:**180–184.
48. **Sainio, M., F. Zhao, L. Heiska, O. Turunen, M. den Bakker, E. Zwarthoff, M. Lutchman, G. A. Rouleau, J. Jääskeläinen, A. Vaheri, and O. Carpén.** 1997. Neurofibromatosis 2 tumor suppressor protein colocalizes with ezrin and CD44 and associates with actin-containing cytoskeleton. J. Cell Sci. **110:** 2249–2260.
49. **Sandsmark, D. K., H. Zhang, B. Hegedus, C. L. Pelletier, J. D. Weber, and D. H. Gutmann.** 2007. Nucleophosmin mediates mammalian target of rapamycin-dependent actin cytoskeleton dynamics and proliferation in neurofibromin-deficient astrocytes. Cancer Res. **67:**4790–4799.
50. **Scherer, S. S., and D. H. Gutmann.** 1996. Expression of the neurofibromatosis 2 tumor suppressor gene product, merlin, in Schwann cells. J. Neurosci. Res. **46:**595–605.
51. **Scoles, D. R., V. D. Nguyen, Y. Qin, C. X. Sun, H. Morrison, D. H. Gutmann, and S. M. Pulst.** 2002. Neurofibromatosis 2 (NF2) tumor suppressor schwannomin and its interacting protein HRS regulate STAT signaling. Hum. Mol. Genet. **11:**3179–3189.
52. **Shaw, R. J., J. G. Paez, M. Curto, A. Yaktine, W. M. Pruitt, I. Saotome, J. P. O'Bryan, V. Gupta, N. Ratner, C. J. Der, T. Jacks, and A. I. McClatchey.** 2001. The Nf2 tumor suppressor, merlin, functions in Rac-dependent signaling. Dev. Cell **1:**63–72.
53. **Sheffield, L. G.** 1998. c-Src activation by ErbB2 leads to attachment-independent growth of human breast epithelial cells. Biochem. Biophys. Res. Commun. **250:**27–31.
54. **Stewart, S. A., D. M. Dykxhoorn, D. Palliser, H. Mizuno, E. Y. Yu, D. S. An, D. M. Sabatini, I. S. Chen, W. C. Hahn, P. A. Sharp, R. A. Weinberg, and C. D. Novina.** 2003. Lentivirus-delivered stable gene silencing by RNAi in primary cells. RNA **9:**493–501.
55. **Sun, C., V. Robb, and D. H. Gutmann.** 2002. Protein 4.1 tumor suppressors: getting FERM grip on growth regulation. J. Cell Sci. **115:**3991–4000.
56. **Tatsumi, Y., Y. Y. Cho, Z. He, H. Mizuno, H. S. Choi, A. M. Bode, and Z. Dong.** 2006. Involvement of the paxillin pathway in JB6 Cl41 cell transformation. Cancer Res. **66:**5968–5974.
57. **Taylor, A. R., S. E. Geden, and C. Fernandez-Valle.** 2003. Formation of a beta1 integrin signaling complex in Schwann cells is independent of rho. Glia **41:**94–104.
58. **Thomas, S. M., and J. S. Brugge.** 1997. Cellular functions regulated by Src family kinases. Annu. Rev. Cell Dev. Biol. **13:**513–609.
59. **Tikoo, A., M. Varga, V. Ramesh, J. Gusella, and H. Maruta.** 1994. An anti-Ras function of neurofibromatosis type 2 gene product (NF2/Merlin). J. Biol. Chem. **269:**23387–23390.
60. **Trofatter, J. A., M. M. MacCollin, J. L. Rutter, J. R. Murrell, M. P. Duyao, D. M. Parry, R. Eldridge, N. Kley, A. G. Menon, K. Pulaski, V. H. Haase, C. M. Ambrose, D. Munroe, C. Bove, J. L. Haines, R. L. Martuza, M. E. Macdonald, B. R. Seizinger, M. P. Short, A. J. Buckler, and J. F. Gusella.** 1993. A novel moesin-, ezrin-, radixin-like gene is a candidate for the neurofibromatosis 2 tumor suppressor. Cell **72:**791–800.
61. **Twist, E. C., M. H. Ruttledge, M. Sanson, L. Papi, P. Merel, O. Delattre, G. Thomas, and G. A. Rouleau.** 1994. The neurofibromatosis type 2 gene is inactivated in schwannomas. Hum. Mol. Genet. **3:**147–151.
62. **Uhlmann, E. J., W. Li, D. K. Scheidenhelm, C. Gau, F. Tamanoi, and D. H. Gutmann.** 2004. Loss of tuberous sclerosis complex 1 (Tsc1) expression results in increased Rheb/S6K pathway signaling important for astrocyte cell size regulation. Glia **47:**180–188.
63. **Wobus, M., R. Kuns, C. Wolf, L. C. Horn, U. Köhler, I. Sheyn, B. A. Werness, and L. S. Sherman.** 2001. CD44 mediates constitutive type I receptor signaling in cervical carcinoma cells. Gynecol. Oncol. **83:**227–234.
64. **Zhu, Y., T. Harada, L. Liu, M. E. Lush, F. Guignard, C. Harada, D. K. Burns, M. L. Bajenaru, D. H. Gutmann, and L. F. Parada.** 2005. Inactivation of NF1 in CNS causes increased glial progenitor proliferation and optic glioma formation. Development **132:**5577–5588.